Ice out of Fire

Ice and cloud condensation nucleation of aerosol particles emitted from controlled soot generation and combustion of renewable fuels

Falk, John

2021

Document Version:
Publisher's PDF, also known as Version of record

Link to publication

Citation for published version (APA):
Falk, J. (2021). *Ice out of Fire: Ice and cloud condensation nucleation of aerosol particles emitted from controlled soot generation and combustion of renewable fuels*. Lund University.

Total number of authors:
1

LUND UNIVERSITY

PO Box 117
221 00 Lund
+46 46-222 00 00

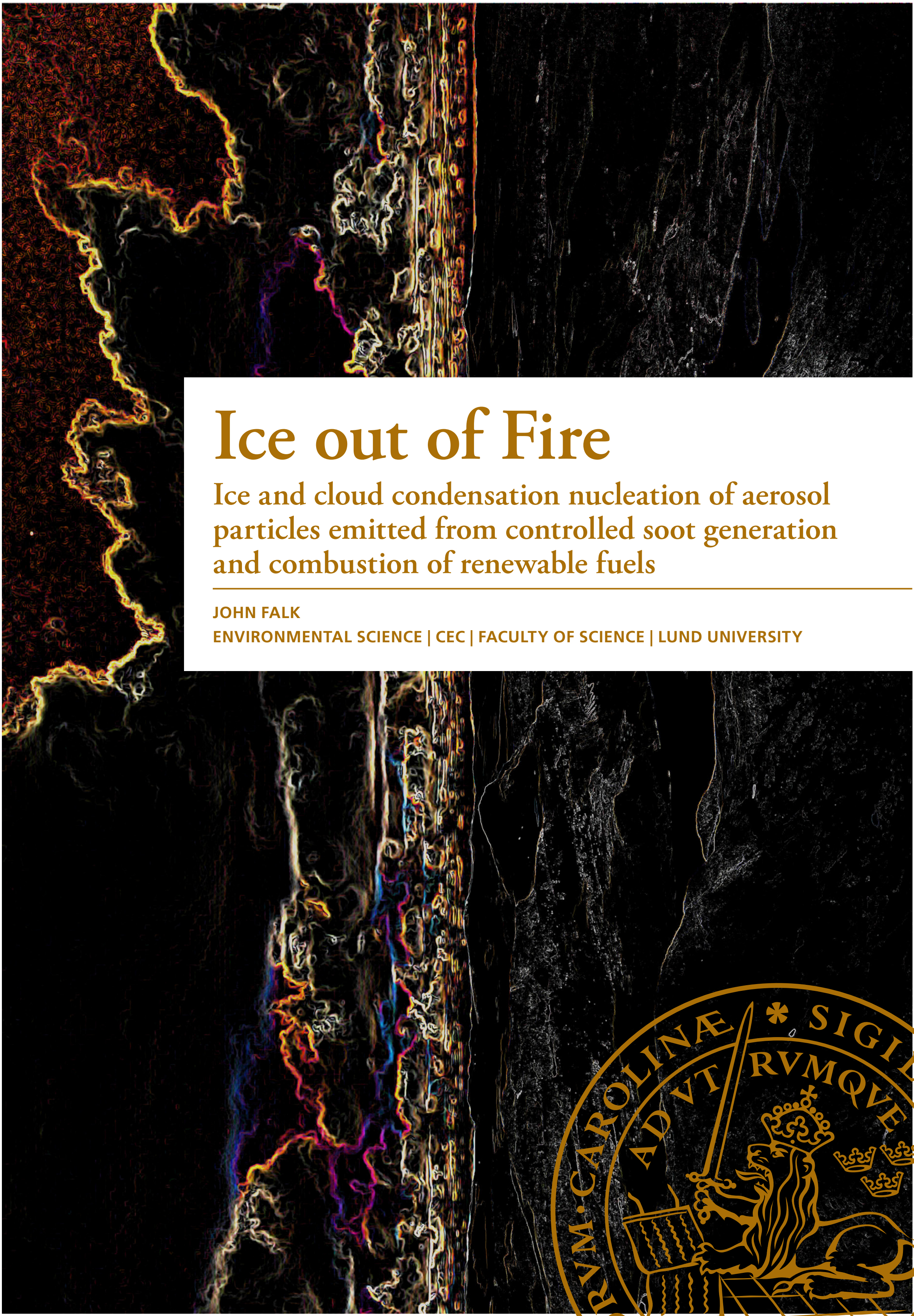

Ice out of Fire

Ice and cloud condensation nucleation of aerosol particles emitted from controlled soot generation and combustion of renewable fuels

JOHN FALK

ENVIRONMENTAL SCIENCE | CEC | FACULTY OF SCIENCE | LUND UNIVERSITY

Ice out of Fire

ICE AND CLOUD CONDENSATION NUCLEATION OF AEROSOL PARTICLES EMITTED FROM CONTROLLED SOOT GENERATION AND COMBUSTION OF RENEWABLE FUELS

I. Immersion freezing ability of freshly emitted soot with various physico-chemical characteristics
Falk, J., Korhonen, K., Malmborg, V.B., Gren, L., Eriksson, A.C., Karjalainen, P., Markkula, L., Bengtsson P.-E., Virtanen, A., Svenningsson, B., Pagels, J., and Kristensen, T.B. *submitted*

II. Immersion freezing ability and characterisation of aged and thermally treated soot
Falk, J., Malmborg, V.B., Nilsson, L., Jakobsson, J., Pagels, J., Kristensen, T.B., and Svenningsson, B. *Manuscript*

III. Particle emissions from a modern heavy-duty diesel engine as ice-nuclei in immersion freezing mode: an experimental study on fossil and renewable fuels
Korhonen, K., Kristensen, T. B., Falk, J., Malmborg, V. B., Eriksson, A., Gren, L., Novakovic, M., Shamun, S., Karjalainen, P., Markkula, L., Pagels, J., Svenningsson, B., Tunér, M., Komppula, M., Laaksonen, A., and Virtanen, A. Atmos. Chem. Phys. Discuss. [preprint], *in review, 2021.*

IV. Ice-nucleating ability of particulate emissions from solid-biomass-fired cookstoves: an experimental study
Korhonen, K., Kristensen, T.B., Falk, J., Lindgren, R., Andersen, Ch., Carvalho, R.L., Malmborg, V., Eriksson, A., Boman, Ch., Pagels, J., Svenningsson, B., Komppula, M., Lehtinen, K.E.J., and Virtanen, A. *Atmos. Chem. Phys.*, 20, 4951-4968, 2020.

V. Properties and emission factors of CCN from biomass cookstoves – observations of a strong dependency on potassium content in the fuel
Kristensen, T.B., Falk, J., Lindgren, R., Andersen, Ch., Malmborg, V.B., Eriksson, A.C., Korhonen, K., Carvalho, R.L., Boman, Ch., Pagels, J., and Svenningsson, B. *Atmos. Chem. Phys.*, 21, 8023–8044, 2021.

Printed by Media-Tryck, Lund 2021 NORDIC SWAN ECOLABEL 3041 0903

LUND
UNIVERSITY

Faculty of Science
Centre for Environmental and Climate Science

ISBN 978-91-7895-958-7

Ice out of Fire

Ice out of Fire

Ice and cloud condensation nucleation of aerosol particles emitted from controlled soot generation and combustion of renewable fuels

John Falk

LUND
UNIVERSITY

DOCTORAL DISSERTATION
by due permission of the Faculty of Science, Lund University, Sweden.
To be defended in the Rydberg hall at the Department of Physics, Sölvegatan 14A, Lund, on
Friday, the 24th of September 2021 at 13:15.

Faculty opponent
Dr. Alexei Kiselev
Institute of Meteorology and Climate Research
Karlsruhe Institute of Technology

Organization
LUND UNIVERSITY

Centre for Environmental and Climate Science (CEC)
Department of Physics, division of Nuclear Physics
Box 118, SE–221 00 LUND, Sweden

Document name
DOCTORAL DISSERTATION

Date of disputation
2021-09-24

Sponsoring organization

Author(s)
John Falk

Title and subtitle
Ice out of Fire: Ice and cloud condensation nucleation of aerosol particles emitted from controlled soot generation and combustion of renewable fuels

Abstract

Aerosol particles, small solid or liquid particles suspended in a gas, are found everywhere in the atmosphere. Air pollution from such particles, mainly soot from combustion-derived activity is a leading cause of premature deaths in the world and have a large effect on the climate. Aerosol particles can interact with climate-related processes in the atmosphere either directly by absorbing or reflecting incoming solar radiation and thus have a heating or cooling effect respectively, or indirectly by influencing clouds which themselves interact with radiation. In the atmosphere all droplets of a cloud form from a subset of existing aerosol particles called cloud condensation nuclei (CCN), and depending on concentration and CCN ability they influence cloud formation and structure, and in turn the climate. Clouds may also consist partly or entirely of ice crystals, which also influences cloud properties and are of special relevance to mixed-phase clouds. For water to freeze at temperatures above -38 °C, an ice nucleating particle (INP) is required. However, the ability of soot to act as such an INP has long eluded the scientific community, and it is still an open question as to why some soot is more efficient as INP than others.

Two laboratory studies were performed on soot generated with a miniCAST soot generator and investigated links between a range of soot physicochemical properties such as chemical composition, soot maturity, optical properties, size and effective density. In the first study, an on-line Continuous Flow Diffusion Chamber (CFDC) was used to investigate immersion and condensation ice nucleation (IN) activity of a wide range of soot maturities from freshly emitted particles. In the other study, an off-line droplet-on-substrate method was used to infer immersion IN activity for a smaller range of soot maturities of fresh and photochemically aged particles. The studies found no significant correlations between soot properties and IN activity, and the results gave indications to that IN related soot particle properties may not be possible to capture with those ensemble measurement methods used.

In a separate laboratory study, immersion and condensation IN activity of combustion emissions from a heavy-duty diesel engine burning low-sulfur fossil diesel, hydrotreated vegetable oil, and rapeseed methyl ester was studied using a CFDC. The IN activity was tested both on freshly emitted as well as photochemically aged soot particles. The study found low to no IN activity from any of the fuels, in line with the current literature.

Two studies were performed on the IN and CCN activity of combustion emissions from various combinations of cook stoves and biomass fuels related to sub-Saharan Africa. Immersion and condensation freezing IN activity was measured with a CFDC, and was moderately IN active in temperatures relevant to mixed-phase clouds. The CCN study showed that primary emission factors have high variability depending on what stove-biomass fuel combination is used, and furthermore depend strongly on the potassium content in the fuel. The results from the study indicate that biomass burning from cook stoves may be an underrepresented source of CCN.

Key words Soot, BC, Immersion freezing, IN, INP, CCN, SPIN, CCNC, MiniCAST, Cold Stage, Cook Stove

Classification system and/or index terms (if any)

Supplementary bibliographical information

Language English

ISSN and key title

ISBN 978-91-7895-958-7 (print)
978-91-7895-957-0 (pdf)

Recipient's notes

Number of pages 185

Price

Security classification

I, the undersigned, being the copyright owner of the abstract of the above-mentioned dissertation, hereby grant to all reference sources the permission to publish and disseminate the abstract of the above-mentioned dissertation.

Signature

Date 2021-08-09

Ice out of Fire

Ice and cloud condensation nucleation of aerosol particles emitted from controlled soot generation and combustion of renewable fuels

John Falk

LUND
UNIVERSITY

Cover illustration: John Falk

Funding information: The project was supported by the Swedish research council FORMAS. Salaries were also covered by faculty funding from Centre for Environmental and Climate Science and from Physics Department at Lund University.

Faculty of Science, Centre for Environmental and Climate Science (CEC)

ISBN: 978-91-7895-958-7 (print)
ISBN: 978-91-7895-957-0 (pdf)

Printed in Sweden by Media-Tryck, Lund University, Lund 2021

Till Mormor
Du är fantastisk

Contents

List of papers included in this thesis

I **Immersion freezing ability of freshly emitted soot with various physico-chemical characteristics**
Falk, J., Korhonen, K., Malmborg, V.B., Gren, L., Eriksson, A.C., Karjalainen, P., Markkula, L., Bengtsson P.-E., Virtanen, A., Svenningsson, B., Pagels, J., and Kristensen, T.B.
[submitted]

II **Immersion freezing ability and characterisation of aged and thermally treated soot**
Falk, J., Malmborg, V.B., Nilsson, L., Jakobsson, J., Pagels, J., Kristensen, T.B., and Svenningsson, B.
Manuscript

III **Particle emissions from a modern heavy-duty diesel engine as ice-nuclei in immersion freezing mode: an experimental study on fossil and renewable fuels**
Korhonen, K., Kristensen, T. B., **Falk, J.**, Malmborg, V. B., Eriksson, A., Gren, L., Novakovic, M., Shamun, S., Karjalainen, P., Markkula, L., Pagels, J., Svenningsson, B., Tunér, M., Komppula, M., Laaksonen, A., and Virtanen, A.
Atmos. Chem. Phys. Discuss. [preprint], in review, 2021

IV **Ice-nucleating ability of particulate emissions from solid-biomass-fired cookstoves: an experimental study**
Korhonen, K., Kristensen, T.B., **Falk, J.**, Lindgren, R., Andersen, Ch., Carvalho, R.L., Malmborg, V., Eriksson, A., Boman, Ch., Pagels, J., Svenningsson, B., Komppula, M., Lehtinen, K.E.J., and Virtanen, A.
Atmos. Chem. Phys., 20, 4951-4968, 2020

V **Properties and emission factors of CCN from biomass cookstoves – observations of a strong dependency on potassium content in the fuel**
Kristensen, T.B., **Falk, J.**, Lindgren, R., Andersen, Ch., Malmborg, V.B., Eriksson, A.C., Korhonen, K., Carvalho, R.L., Boman, Ch., Pagels, J., and Svenningsson, B.
Atmos. Chem. Phys., 21, 8023–8044, 2021

All papers are reproduced with permission of their respective publishers.

Author's contributions to the papers included in this thesis

Paper I: Immersion freezing ability of freshly emitted soot with various physico-chemical characteristics

I participated in planning the experiment. I performed the measurements with co-authors, and was responsible of operating the MiniCAST and APM. I analysed SPIN, SMPS, APM, Aethalometer data, and contributed to AMS data analysis. I interpreted the data and wrote the manuscript with contributions from co-authors.

Paper II: Immersion freezing ability and characterisation of aged and thermally treated soot

I was responsible for formulating the research question and planning the experiment. I was responsible for overseeing and executing the measurements, as well as the operation of the APM, SMPS, CCNC, Aethalometer and miniCAST instruments. I was responsible for preparing, collecting and analysing the filter samples. I was responsible for analysing all instrument data except AMS. I wrote the manuscript with contributions from co-authors.

Paper III: Particle emissions from a modern heavy-duty diesel engine as ice-nuclei in immersion freezing mode: an experimental study on fossil and renewable fuels

I contributed to the experiment planning. I shared responsibility of performing the measurements, and was responsible for operating the APM and CCNC instruments. I performed analysis of APM data. I contributed to the uncertainty analysis of the SPIN instrument data.

Paper IV: Ice-nucleating ability of particulate emissions from solid-biomass-fired cookstoves: an experimental study

I performed analysis of DMS and SMPS data. I performed CCNC instrument calibration. I contributed to SPIN data uncertainty analysis. I made contributions to the interpretation of data. I made minor contributions to the writing of the manuscript and the peer-review process.

Paper V: Properties and emission factors of CCN from biomass cookstoves – observations of a strong dependency on potassium content in the fuel

I performed the analysis of CCNC, DMS and SMPS data. I Performed the CCNC instrument calibration. I carried out compilation and analysis of data to obtain CCN emission factors. I contributed to the interpretation of data. I also contributed to writing and the peer-review process.

Populärvetenskaplig sammanfattning

Mänsklig aktivitet leder till betydande mängder luftföroreningar, av konsekvens för både jordens klimat och människors hälsa. Av särskild vikt är de partiklar från förbränning som släpps ut i vår närhet och atmosfär, och som är kopplade till en rad hälsoproblem så som luftvägsinfektioner, lungcancer och hjärt- och kärlsjukdomar. Till följd av dessa luftföroreningar dör varje år nästan sju miljoner människor i förtid, och även om människor överallt på jorden påverkas av detta, så är befolkningen i utvecklingsländer särskilt utsatta. Omkring hälften av jordens befolkning, främst i Afrika och Asien, är nämligen beroende av förbränning av biomassa eller restprodukter från jordbruk för att kunna laga mat eller ha tillgång till värme och belysning. Oftast sker denna förbränning dessutom inomhus vilket leder till större exponering av dessa skadliga partiklar.

Globalt sett kommer den största andelen luftföroreningar från förbränningsprocesser orsakade av människan. Exempelvis är eldning i bostäder, fordonsmotorer och utsläpp i samband med industriell produktion vanliga källor, men även naturligt orsakade vegetationsbränder leder till stora utsläpp. Vid de höga temperaturer som råder under förbränning bildas små partiklar vilka till största delen består av kol, så kallade sotpartiklar. De flesta av dessa brinner upp, men en del släpps ut till omgivningen. Sotpartiklar absorberar ljus, eller strålning, vilket ger dem den karakteristiska svarta färg vi också vanligtvis förknippar med sot. Den strålning som tas upp av sotpartiklarna skickas ut igen i form av värmestrålning, och på grund av de stora mängder sotpartiklar som ständigt finns i atmosfären bidrar detta till en kraftigt uppvärmande effekt av jorden. Egenskaperna hos de sotpartiklar som bildas varierar dock beroende på förhållandena under förbränningen, och i vissa fall bildas sotpartiklar vars klimatpåverkan är mer svårtolkad.

Molnen i vår atmosfär förser oss inte endast med vackra och ibland häpnadsväckande vyer, utan spelar också en väldigt viktig roll för livet på jorden. De förser genom nederbörd jordens landmassor med det vatten som blir grundvatten, sjöar och andra vattendrag och som växt- och djurliv behöver för att leva. Moln är också viktiga för jordens energibalans eftersom de små partiklar - droppar eller iskristaller - som molnen är uppbyggda av också interagerar med strålning från både solen och jorden. Molnpartiklarna sprider solens inkommande strålning och reflekterar på så vis en stor del tillbaks ut i rymden. Motsvarande effekt sker med den värmestrålning som jorden avger, och på nätter värmer molnen i stället upp jorden genom att reflektera tillbaks denna strålning mot jorden.

För att molndroppar ska kunna bildas från den vattenånga som finns i atmosfären så behövs en redan befintlig flytande eller fast partikel på vilken ånga kan kondensera. Utan en sådan partikel, oftast omkring några tiotusendels millimeter stor, skulle droppbildningen behöva starta från små kluster av vattenmolekyler, vilket kräver mycket hög övermättnad av vattenånga. Alla partiklar bidrar inte till att molndroppar bildas, utan det krävs att partiklarna helt eller delvis är hygroskopiska, det vill säga består av ämnen som vill ta åt sig vatten, till exempel olika salter.

Vatten fryser inte nödvändigtvis till is när temperaturen är under smältpunkten, utan kan hålla sig i flytande form i minusgrader, då kallat underkylt vatten. I atmosfären fryser vattendroppar först vid -38 °C, och för att vattnet skall bilda is ovan denna temperatur så krävs det en fast yta, små orenheter med egenskaper som gör det lättare för is att bildas på dem. Vissa partiklar i atmosfären har sådana egenskaper och kan bilda is från underkylt vatten på flera olika sätt, men även under vissa förutsättningar också direkt från vattenånga. När is bildas i ett moln påverkar det molnets egenskaper, och över land är det till exempel oftast isbildning som leder till nederbörd. Även om där är ett ytterst litet antal av alla partiklar i atmosfären som är isbildande, så kan de ha en stor effekt på molnen, och som konsekvens, klimatet.

Sotpartiklar är generellt väldigt vattenavstötande, men både förbränningsförhållanden och atmosfärsik åldring kan leda till att de lättare tar åt sig vatten. Atmosfärisk åldring innebär att kemiska processer i atmosfären påverkar sammansättningen, och sker även för andra typer av partiklar. Av särskilt intresse är dock sotpartiklar med avseende på isbildning, eftersom dessa egenskaper fortfarande är oklara. Många olika studier har gjorts på sotpartiklars isbildningsförmåga, men få verkar ge överrensstämmande resultat. På senare tid har det i huvudsak rapporterats att sotpartiklar i allmänhet verkar vara ineffektiva på att bilda is.

I denna avhandling har olika laboratoriestudier utförts för att öka den grundläggande förståelsen för hur olika sotpartikelegenskaper relaterar till isbildningsförmåga. Laboratoriestudier har även utförts med syfte att studera just molndroppsbildning och ispartikelbildning hos partiklar från olika förbränningskällor kopplade till mänskliga utsläpp.

Studier kring hur olika egenskaper hos sotpartiklar påverkar ispartikelbildning genomfördes med en flamsotsgenerator för både färskt producerade samt åldrade partiklar. Resultaten visade på en generellt mycket låg nivå av isbildning, i enlighet med andra nyligen publicerade studier. Både fysiska och kemiska partikelegenskaper försökte kopplas till isbildning, men inga tydliga samband kunde hittas. Resultaten indikerar att de metoder som använts för att studera partikelegenskaper kanske inte har möjlighet att mäta de egenskaper som ger upphov till isbildning.

Mätningar på sotpartiklarna som släpps ut från en dieselmotor visar på överlag insignifikant isbildningsförmåga för både fossilt och förnyelsebara bränslen. Små skillnader kan synas mellan bränslen, men resultaten är i enlighet med tidigare studier som visar att partiklar från dieselmotorer inte är särskilt isbildande.

Partiklar från biomassförbränning är med sannolikhet av vikt för klimatet med avseende på både molndroppsbildande och isbildande partiklar. Mätningar genomfördes på en rad olika spisar och biomassabränslen av särskild relevans för subsahariska Afrika, och studierna visade att det antal molndroppsbildande partiklar som släpps ut under förbränning kan variera kraftigt beroende på val av spis så väl som bränsle, samt om de åldrats i atmosfären. Även partiklar med tämligen isbildande förmåga bildades i de flesta av mätningarna, och med avseende på det stora antal människor som världen över behöver förlita sig biomassförbränning så är det viktigt att fortsätta lära oss mer om denna källa.

Klimatkrisen är ett faktum, och vi vet idag tillräckligt mycket för att agera och minska de utsläpp av växthusgaser vi orsakar. För att mer effektivt kunna motverka vår klimatpåverkan är det dock viktigt att vi ökar vår kunskap kring hur de olika förbränningspartiklar som släpps ut påverkar klimatet. Arbetet i denna avhandling har för avsikt att bidra till denna kunskap.

Ice out of Fire: Ice and cloud condensation nucleation of aerosol particles emitted from controlled soot generation and combustion of renewable fuels

List of abbreviations

BC	black carbon
CCN	cloud condensation nuclei
CCNc	cloud condensation nuclei counter
CFDC	continuous flow diffusion chamber
DMA	differential mobility mass analyser
DOC	diesel oxidation catalyst
DPF	diesel particulate filter
ED	ejector diluter
GHG	green house gases
IN	ice nucleation
INP	ice nucleating particle
LUCS	Lund University Cold Stage
MPC	mixed-phase clouds
OFR	oxidation flow reactor
PAH	polycyclic aromatic hydrocarbon
PAM	Potential Aerosol Mass chamber
PCF	pore condensation freezing
PM	particulate Matter
PTD	porous tube diluter
RF	radiative forcing
RH	relative humidity
SOA	secondary organic aerosol
SPIN	SPectrometer for Ice Nucleation
TD	thermodenuder

1 Introduction

1.1 Combustion emissions, air pollution and clouds

Humans have a profound impact on the Earth, and have had so for thousands of years. Ever since the start of the 18th century, rapid population growth and industrialisation have increasingly made it visible how we influence all of the Earth's natural systems. Anthropogenic activity influences everything from remote marine ecosystems (Halpern et al., 2008) to our own life expectancies (Landrigan et al., 2018). It is even debated as to whether or not human influence on the Earth should be considered the defining property of our current geological epoch, informally calling it the Anthropocene (Crutzen, 2002). Industrial activity and everyday living is coupled to air pollution across the globe. Be it for transport, production, residential heating or cooking, we release large amounts of gaseous and particulate matter (PM) into the Earth's atmosphere - and in the case of many developing regions - into our homes.

PM is made up of aerosol particles, and are liquid or solid particles suspended in the air. They can be anywhere from a few nanometers to several micrometers in diameter, and with vastly different shapes. The adverse health effects of air pollution has been known since at least the mid 20th century, when smog episodes in Donora, PA (1948) and London, UK (1952) showed strong links between exposure to heavily polluted air, human disease and death (Costa, 2018). While these episodes increased awareness on the issue of ambient air pollution, it was not until the seminal Six Cities Study by Dockery et al. (1993) that a clear, general correlation could be made between levels of particulate air pollution and negative health effects. The study followed the health status of 8111 white adults in six different US cities during a period 14 to 16 years, and concluded that fine PM or PM2.5 - PM of an aerodynamic diameter smaller than 2.5 micrometer - present in the air led to increased mortality rates, lung cancer and cardiopulmonary diseases.

Today, ambient air pollution and household air pollution is linked to close to 7 million premature deaths per year according to most recent global estimates, with household air pollution accounting for around 40 % of those deaths (Landrigan et al., 2018; WHO, 2016; HEI, 2020). While air pollution affects all regions of the world, low-middle income regions primarily in Asia and Africa are disproportionately affected, and a majority of the premature deaths attributed to household air pollution come from these regions (HEI, 2020). An estimated 2.8 - 4 billion people around the world, mainly in these regions, rely on burning solid fuels such as biomass or agricultural residue for everyday cooking, lighting and heating (ESMAP, 2020; IEA et al., 2020).

The most well understood and quantified climate related effects of air pollution come from greenhouse gases (GHGs) such as CO_2, CH_4 and halocarbons. In the 1960s and 70s, a series of seminal studies were published showing annually rising levels of the GHG CO_2 in the atmosphere (Pales and Keeling, 1965; Keeling, 1973; Keeling et al., 1976). While not the first studies of its kind (Callendar, 1938), the results of rising CO_2 concentrations provided for the first time clear evidence of how the Earth's atmosphere is directly polluted by mainly anthropogenic combustion of fuels, and subsequently in the following decades helped establish the scientific consensus on humanity's role in climate change. GHGs interact directly with thermal infrared radiation in the atmosphere, causing a build-up of heat energy within the atmospheric layer (Rhein et al., 2013). According to the most recent IPCC assessment report estimates, anthropogenic GHGs are the major contributor to the positive net change in the Earth's energy balance, or radiative forcing (RF). Combined, the increased concentrations of anthropogenic GHGs since the start of the industrial age have led to an increased RF of +2.83 (2.54 to 3.12) Wm^{-2}. (Myhre et al., 2013). However, as illustrated in Figure 1, GHGs are not the only anthropogenically emitted compounds affecting RF, and the largest uncertainties are attributed to aerosol particle emissions. There exist additional complex relationships between the various gaseous and particulate emissions introduced into the atmosphere and their influence on the Earth's climate system, obscuring the overall impact of specific emissions.

Depending on species and atmospheric conditions, gaseous emissions can condense onto existing or form new aerosol particles, and how these particles interact with the climate system depend significantly on their resulting physical and chemical properties. Sulfate particles for example, formed in majority from chemical reactions in the atmosphere from sulfur dioxide emissions of both natural sources such as volcano eruptions or combustion of sulfur-rich fuels such as coal, reflect solar radiation and have a negative RF and thus a cooling effect on the Earth. However, soot particles which have a net positive RF and a warming effect on the climate much like GHGs, have been shown to have their effect increased when coated with sulfates (Moffet and Prather, 2009), causing sulfates to indirectly also lead to a warming effect.

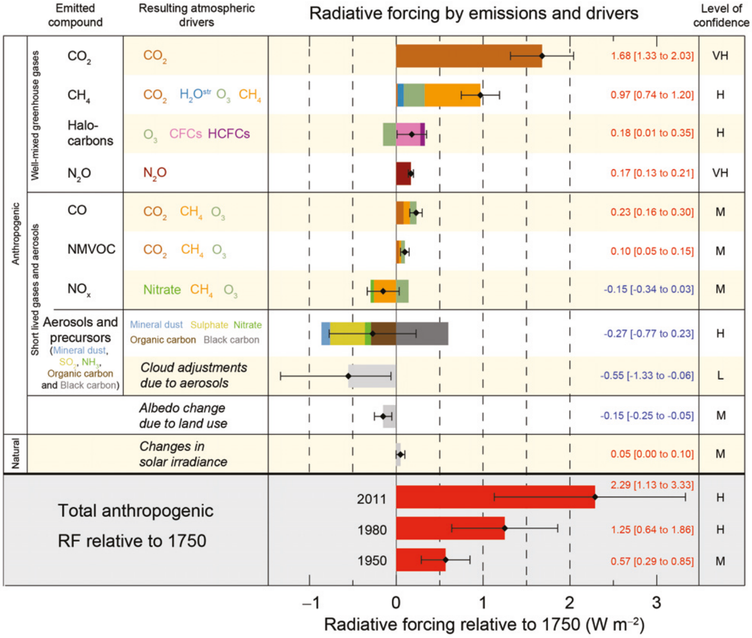

Figure 1: Originally published in the IPCC AR5 (IPCC, 2013). Estimated increase of radiative forcing between 1750 - 2011 from individual anthropogenically emitted compounds. Note the large uncertainties associated with aerosols and precursors, and especially cloud adjustments from aerosol particles.
Original figure text: Radiative forcing estimates in 2011 relative to 1750 and aggregated uncertainties for the main drivers of climate change. Values are global average radiative forcing (RF[14]), partitioned according to the emitted compounds or processes that result in a combination of drivers. The best estimates of the net radiative forcing are shown as black diamonds with corresponding uncertainty intervals; the numerical values are provided on the right of the figure, together with the confidence level in the net forcing (VH – very high, H – high, M – medium, L – low, VL – very low). Albedo forcing due to black carbon on snow and ice is included in the black carbon aerosol bar. Small forcings due to contrails (0.05 Wm^{-2}, including contrail induced cirrus), and HFCs, PFCs and SF 6 (total 0.03 Wm^{-2}) are not shown. Concentration-based RFs for gases can be obtained by summing the like-coloured bars. Volcanic forcing is not included as its episodic nature makes is difficult to compare to other forcing mechanisms. Total anthropogenic radiative forcing is provided for three different years relative to 1750. Reprinted with permission from IPCC (2013).

Clouds play an important role in the Earth's climate, and aerosol particles have a potentially significant indirect effect on the climate through influencing cloud formation and structure. Clouds are made up of small liquid droplets, ice crystals or both. In the atmosphere, these cloud droplets are initially formed through water vapour condensing onto some of these aerosol particles, called cloud condensation nuclei (CCN). The science behind CCNs is further detailed in subsection 3.2. The science behind what properties makes an aerosol particle a CCN in atmospheric conditions is well-known, however due to the vast amount of different types of particles emitted, and how they from chemical reactions may change in the atmosphere, makes it non-trivial to assess how the various sources may affect the climate.

How ice crystals form in the atmosphere is a bit more complex. They may form directly from a liquid droplet freezing in the atmosphere which requires temperatures of less than

-38 °C. Ice can form in sub-zero temperatures warmer than this, however for this to happen, ice nucleating particles (INPs) must be present. These processes are discussed more in subsection 3.3. Not as much is known about the ice nucleating properties of aerosol particles, and while many types of aerosol particles have been identified as effective INPs, such as dusts from deserts, arid soils and volcanic eruptions or bioaerosols such as bacteria and pollen, the role of soot particles remain uncertain. Known INPs are relatively rare in atmosphere, on average on the order of one INP per 10^5 particles but can assert a disproportionate influence on clouds. The ice nucleating ability of soot is thus, due to the large global anthropogenic and natural emission quantities, of importance to more reliably understand and predict cloud processes and its subsequent effect on Earth's climate.

1.2 Thesis aims

The overall aim of this thesis was to investigate how anthropogenic combustion particles influence cloud properties and climate. The aims based on this were to: 1) investigate INP and CCN activity from aerosol particles emitted from renewable fuel based real-world sources, 2) identify what physico-chemical soot particle properties may govern immersion freezing ice nucleating ability, and 3) put these results into a climate-relevant context. The specific aims of this thesis were to investigate knowledge gaps in relation to:

I: Whether it is possible from online ensemble measurement methods to identify any physico-chemical properties from generated soot which correlate with immersion freezing ice nucleating activity. (Paper I & II)

II: How ice nucleation activity of soot post-combustion is affected by any combination of 1) removal of volatile surface compounds and 2) photochemical ageing, as well as photochemical ageing alone. (Paper II)

III: The immersion ice nucleating activity of combustion particles emitted from a range of renewable fuel combustion sources related to real-life sources. (Paper III & IV)

IV: How combustion and fuel chemical composition for a range of biomass solid fuels and cook stove technologies influence particles emission cloud condensation nuclei properties and emission factors. (paper V).

2 The many faces of soot

2.1 Soot formation and characteristics

Carbonaceous soot particles form through a series of complex processes in fuel-rich, high temperature environments, where unburned fuel in the gas-phase undergo reactions and subsequently nucleates into the solid-phase. This formation can generally be regarded as happening through a five step process: pyrolysis, nucleation, surface growth, coalescence and agglomeration, all of which occurs under very short time-scales (Tree and Svensson, 2007). Pyrolysis is a process occurring under high temperature conditions, in which organic compounds such as hydrocarbons (HC) in solid or liquid fuels undergo reactions altering their molecular structure and giving rise to new compounds. Apart from fuel chemical composition, due to the generally endothermic nature of these reactions the resulting products are highly temperature dependent (Smith, 1981). The fuel pyrolysis leads to a number of different gas-phase HC compounds, some of which react to form or grow polycyclic aromatic hydrocarbons (PAHs), which are known to be soot precursors (Homann, 1998; Frenklach, 2002; Wang, 2011). Unsaturated HCs, especially acetylene and propargyl are thought to have a central role in these processes, and acetylene especially in the build-up of larger aromatic structures (Tree and Svensson, 2007; Glassman, 1989; Richter and Howard, 2000).

The nucleation of soot particles occurs when these larger aromatic molecules transition from the gas-phase into molecule clusters, or incipient soot particles of a few nanometers in size. While the pathways governing the formation of these particles are still not completely understood, a few mechanisms have in recent years been proposed (Wang, 2011; Johansson et al., 2018; Frenklach and Mebel, 2020). These incipient soot particles account for a small proportion of the total soot mass, but have a large influence on the mass added later.

The incipient soot particles continue to grow after nucleation, and there is not clear distinction between where nucleation ends and surface/mass growth begins. The hot particle surface reacts with H and OH radicals which create reactive sites onto which gaseous species, particularly acetylene, can be added causing the soot particle to grow. While growing, two incipient soot particles may coalesce, resulting in two roughly spherical particles combining to form a single larger, likewise roughly spherical particle. These processes lead to refractory so-called primary particles, which generally are on the order of tens of nanometers in size (Frenklach, 2002; Baldelli et al., 2020). These primary soot particles are often characterized by having a disordered inner core, and a more ordered outer shell, where the core is associated with the incipient soot particle, whereas the shell is associated with the subsequent growth of the particle. The actual structure of these regions depend strongly on combustion conditions in the flame such as pressure, temperature and fuel composition (Kholghy et al., 2016). Oxidation of the soot particle surface occurs all throughout as well as after soot particle formation, however the levels of oxidation may vary to a large degree depending on combustion conditions. It reduces the mass of the particle by converting parts of its mass back into the gas-phase, e.g. to CO_2 and CO and in for example modern diesel engines, a majority of the soot is oxidized away during combustion. Oxidation of the particles lead to surface oxides, which alter surface properties of the soot particle (Figueiredo et al., 1999; Corbin et al., 2015). The oxidant elements depend on combustion conditions, and for example in a modern diesel engine OH may act as a principal oxidant (Gallo et al., 2017).

The primary particles undergo agglomeration during and after the combustion. This is the process in which multiple primary particles stick together to form a larger soot particle sometimes referred to as a soot aggregate, while keeping their individual primary particle structure (Frenklach, 2002). The process is separate from the previously mentioned coalescence process, where two incipient particles combine to form a new spherical particle. Agglomeration leads to the fractal or chain-like structures, as can be seen in Figure 2, often associated with soot particles.

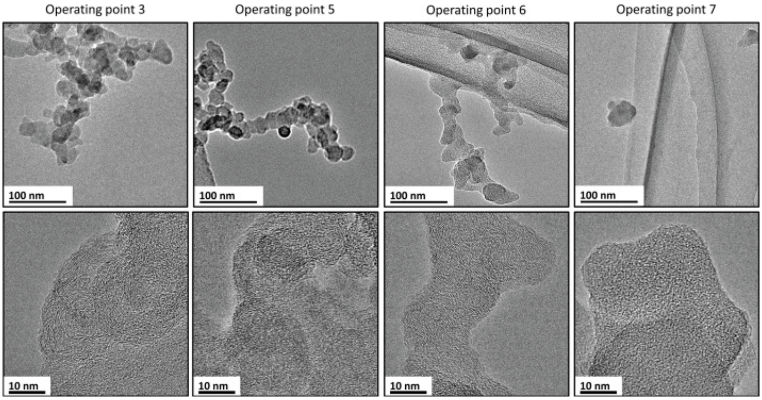

Figure 2: Originally published in Malmborg et al. (2019). High-resolution transmission electron microscopy images of soot particles from a miniCAST flame soot generator (see section 4.1). The different columns, named *operation points* in the figure, represent different combustion conditions. The upper row shows the larger agglomerate structure, and the lower row shows the nanostructure of each primary particle, both dependent on combustion conditions. Copyright Malmborg et al. (2019). Licensed under Creative Commons CC-BY 4.0 (https://creativecommons.org/licenses/by/4.0/).

Soot maturity is a measure of the amount of time the soot particles spend in the high-temperature regions of the flame, which affects their carbon structure and chemical composition. Partially mature soot has a structure consisting to a larger degree of organic carbon, such as saturated or unsaturated hydrocarbons, PAHs, and oxidized organics. As the soot matures, in combination with oxidation, coagulation and surface growth processes, its primary particle carbon structure transitions from a more amorphous arrangement into a more elemental carbon containing micro-crystalline graphite-like and onion-layered structure as well as fragmenting or reducing in size (Lahaye and Prado, 1981; Harris and Weiner, 1983; Kholghy et al., 2016).

In the atmosphere, soot particles are subject to a number of processes commonly referred to as atmospheric processing or atmospheric ageing, further changing their structure and chemical composition and potentially affecting for example hygroscopicity and optical properties (Zhang et al., 2008; Liu et al., 2010; Xue et al., 2009), and may influence ice nucleating ability (Mahrt et al., 2018). These processes include adsorbtion of gaseous organic species (Saathoff et al., 2003), coagulation with other existing particles such as secondary organic aerosols (SOA), nitrates and sulfates, and photochemical oxidation.

2.2 Atmospheric sources of soot

Soot is present throughout the atmosphere, and originates from incomplete combustion by both anthropogenic and natural sources. Black carbon (BC) is the most common metric in assessing regional and global quantities of atmospheric soot, and is often used synonymously with the term soot to describe the carbonaceous graphite-like material formed from combustion. BC is an operationally defined quantity based on the mostly wavelength independent highly light-absorbing characteristics of soot.

BC has a rather short lifetime estimated to be in the range of from days to weeks in the atmosphere (Ramanathan and Carmichael, 2008; Cape et al., 2012) under which it can be transported in the atmosphere in excess over 1000 km from its source (Rodhe et al., 1972; Byčenkienė et al., 2011) before being removed due to wet (e.g. in precipitation) or dry (e.g. gravitational sedimentation) deposition processes. However, a more recent modelling study by Lund et al. (2018) have found that lower lifetime constraints than previous estimates were required to align model estimates with observations, indicating that previous transport estimations might be overestimated.

Anthropogenic sources are currently estimated to account for more than 75 % of total global BC worldwide (Klimont et al., 2017), and are in majority due to combustion of fossil and biomass fuels including agriculture, transport, energy production and residential combustion (Bond et al., 2013; Klimont et al., 2017). Natural sources are mainly due to open burning of vegetation such as wildfires. An overview of global BC emission rates by source category and region for the year 2000 can be viewed in Figure 3. Current modelling estimates indicate a global increase of yearly BC emissions, although to a varying degree. Klimont et al. (2017) reported an increase of 15 % in global BC emissions between 1990 and 2010, mostly attributed to the growth of emissions in Asia and Africa (30 and 40 %, respectively). Comparatively, during the same period emissions in Europe, North America and Pacific declined by around 30 % despite the global increase. These numbers highlight the rather large difference in regional burden of BC emissions.

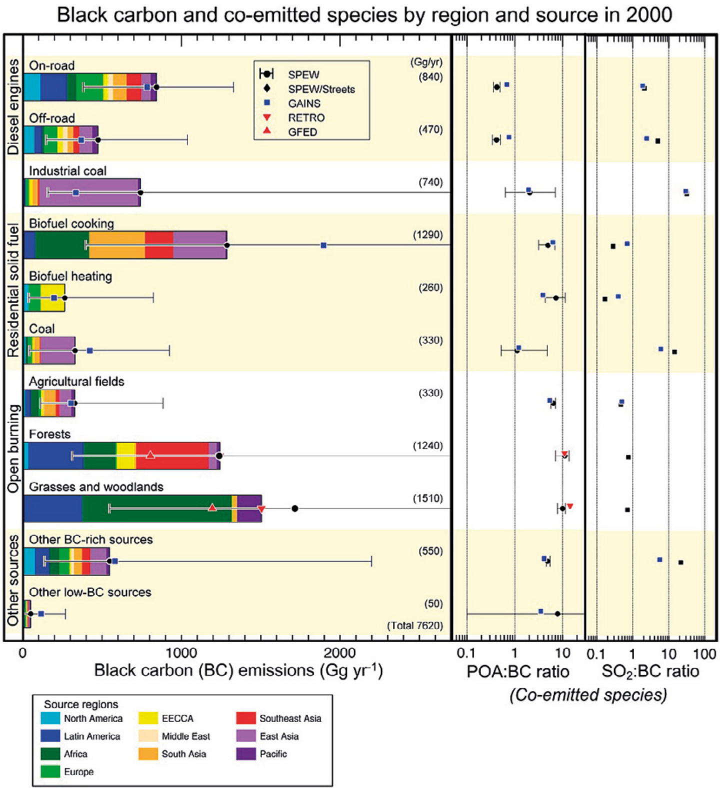

Figure 3: Originally published in Bond et al. (2013). Black carbon emission rate estimates in $Gg\ yr^{-1}$ for the year 2000, categorised by source and region. Visible here are the large contributions of BC from the residential solid fuel category, mainly attributed to Africa and Asia regions. Open fires in this figure include fires purposefully or involuntarily caused by humans. ©Bond et al. (2013). Licenced under Creative Commons CC-BY-NC-ND 3.0 (https://creativecommons.org/licenses/by-sa/3.0/).

Brown carbon (BrC) is also an important component of incomplete combustion emissions. BrC are carbonaceous light-absorbing particles with an overall weaker absorption compared to BC, characterised by enhanced absorption at shorter relative to longer wavelengths. BrC originate from both primary and secondary sources, with biomass or biofuel combustion being major primary sources (Andreae and Gelencsér, 2006; Laskin et al., 2015). Secondary sources are related to atmospheric processing of compounds associated with biogenic sources and biomass combustion emissions, and may also comprise of humic-like substances. (Andreae and Gelencsér, 2006; Lack et al., 2013; Laskin et al., 2015). BrC particles are chemically very complex and therefore also more difficult to assess in a climate relevant context especially as to their indirect effects, however they are estimated to account for a substantial portion of carbonaceous aerosols direct radiative forcing (Zhang et al., 2017; Zeng et al., 2020).

Each source has different implications owing not only to the different characteristics of the emitted particles, but also the immediate environment in which they are emitting. For example, while BC emissions from aviation constitute about one percent of global anthropogenic total, it may be an important direct source of influence on clouds in the upper troposphere (Popovicheva et al., 2004; Kärcher, 2018). The largest source of anthropogenic BC globally is residential combustion (Bond et al., 2013; Klimont et al., 2017). This category is dominated by biomass combustion used for cooking, heating and lighting, and is mostly attributed to regions in Africa and Asia where few to no viable alternative energy sources exist.

2.3 Soot sources in developing regions

It is estimated that about 2.8 to 4.0 billion people around the world, predominantly in developing regions such as sub-Saharan Africa and south-east Asia rely on residential combustion from traditional cook stove technology and fuels for their everyday cooking, lighting and heating needs (IEA et al., 2020; ESMAP, 2020). Traditional cook stoves, often represented by a simple three-stone fire are less energy efficient and emit large amounts of gases and aerosol particles compared to clean technology and fuel alternatives. Since cook stoves are generally located inside of homes, they are a leading contributor to household air pollution which is estimated to lead to around 3-4 million premature deaths per year globally (Forouzanfar et al., 2016). Women and children are disproportionately exposed to household air pollution, as women are generally in charge of traditional household duties such as cooking and childcare (Clougherty, 2010; Smith et al., 2014). Due to the large scale of cook stove usage, residential combustion is a leading driver of BC emissions not only regionally but also globally. In a modeling study by Lacey et al. (2017), which studied the global climate and health impact of cook stove emission reductions, it was estimated that a gradual phasing out of cook stove emissions by 2050 could lead to roughly a tenth of a degree reduction in global temperature increase, as well as a significant reduction in global preventable deaths per year. However, the large uncertainty in how aerosol particles from these sources may act as CCN or IN in the atmosphere complicates the process of establishing high confidence policy measures as for example in relation to the United Nations Sustainable Development Goal 7, of taking urgent action to combat climate change and its impacts. Access to cleaner cook stove technologies and fuels has been slowly increasing globally in the last decade, from 56 to 63 % between 2010 - 2018 (UN. Secretary-General, 2020). However, this trend of access is not true for sub-Saharan Africa where due to the rapid population increase in the region access to clean cook stove technology and fuels have instead decreased. In 2014, 82 % in sub-Saharan Africa, or about 730 million people relied on the use of traditional solid-fuel biomass such as wood, agricultural residue or dung for energy, out of which 80 % is used for household cooking in the region due to the large reliance (75 %) on traditional, energy-inefficient cook stove types such as the three-stone fire (IEA, 2014; World Bank, 2014).

3 Clouds

3.1 What is a cloud?

Although to the layperson often thought of as a kind of gas, a cloud is actually an aerosol which is made up of both gaseous matter, and particles suspended in it. The most fundamental parts of the cloud are the vast amount of small liquid water or ice crystal particles it contains, which is also what we see when we look at them. Generally these particles are in the range of 5 to 50 micrometers in size, but there are many factors governing their size and growth. If they grow large enough, they will begin to fall towards the Earth surface as rain. Clouds play an important role in the hydrological cycle via water transport and precipitation, and have a significant effect on the radiative forcing on the Earth Boucher et al. (2013). Out of the on average 340 Wm^{-2} of solar radiation that reaches the Earth, clouds reflect about 20 % back into space, more than the Earth's surface would in the absence of clouds. They also have an effect of keeping a portion of the long-wave radiation emitted by the Earth surface from escaping the atmosphere.

Clouds can start to form when the water vapour partial pressure of a given air volume becomes greater than the saturated partial vapour pressure with respect to liquid water or ice, respectively. Under these conditions, the volume gets supersaturated with water vapour, equivalent to a reaching a relative humidity (RH) of above 100 %. The level of supersaturation is most commonly presented as the percentage above 100 % RH. However, droplet formation in homogeneous water vapour would require a RH_{water} on the order of several hundred percent %, and is virtually impossible under atmospheric conditions. Instead, in order for water vapour to condense into liquid phase and form droplets, and consequently clouds, there needs to be a pre-existing solid or liquid particle present - a CCN - onto which the vapour can start to condense. This section covers the formation of clouds on the macro-scale, and the topic of CCN is further explored in subsection 3.2. Somewhat analogous to CCN, cloud ice crystals also require a pre-existing particle in order to allow formation under atmospherically relevant supersaturation conditions, and is explored in subsection 3.3.

The amount of water vapour an air volume can contain without being supersaturated is dictated by temperature, where a lower temperature leads to a lower water vapour capacity. This means that clouds may form via a change in any of these two variables: Temperature or water vapour content. A common quantity describing this is the dew point, which is the temperature at which water vapour in a given air volume becomes saturated for a given air pressure and water vapour content. In the atmosphere, this may happen in several ways. A common way in which clouds form is via adiabatic cooling, and occurs when an air volume is lifted and exposed to a lower pressure environment, causing expansion and subsequent cooling of the volume. This lift can be initiated from orographic lift, frontal lift, convergence or convective lift. Orographic lift is when the air volume is moving along rising geographical features such as mountains. Frontal lift happens when one air volume meets another of a different temperature, causing the warmer volume to go above and over the colder volume. Convergence happens in the center of low pressure areas, where the surrounding higher pressure areas force the low pressure air to rise. Convective lift is the most common process, in which the buoyancy of an air volume at the surface is increased from warming in relation to the surrounding air, causing it to rise. Water vapour saturation of a given air volume can also be reached from non-adiabatic cooling, via conductive, radiative or evaporational cooling. It can also occur if the water vapour content is added from adjacent sources, such as from moist surfaces, precipitation or plant transpiration. These two latter are most common at the surface level, resulting in haze or fog.

Clouds are most often found in the troposphere, but may under some circumstances also form higher up, in the form of polar stratospheric or mesospheric clouds (Tritscher et al., 2021). The latter have also been implicated to be an indicator for climate change (Lübken et al., 2018) due to the increasing concentrations of CO_2 and H_2O in the atmosphere. In the troposphere clouds appear in a wide range of different shapes and configurations, and have a rather extensive taxonomy related to them. At the highest taxonomy level there are ten types of clouds classified based on cloud physical shape and process of formation, as well as at which height level they commonly form in: High, middle or low. These heights naturally vary depending on longitudinal climate differences, and clouds classified as high clouds in tropical regions may occur at much higher altitudes than in polar regions. The ten types of clouds are depicted in Figure 4. High level clouds occur at around 5 - 13 km in temperate regions (about 3 - 8 km in polar, 6 - 18 km in tropical regions), and include cirrus, cirrostratus and cirrocumulus clouds. These clouds types are all predominantly made up of ice crystals, and have a somewhat transparent, often whispy and fibrous appearance. Middle level clouds occur at around 2 - 7 km in temperate regions (2 - 4 km in polar, 2 - 8 km in tropical regions), and include altocumulus, altostratus and nimbostratus clouds. Altocumulus clouds often have the appearance of many smaller, tightly arranged opaque white clouds. The latter two are most often found in the middle level, but altostratus may extend to the high level and nimbostratus may extend to both high and low levels. They are rather featureless, often greyish cloud sheets and nimbostratus is additionally often associated with rain. Low level clouds occur at around 0 - 2 km in all regions, and include stratus clouds, which are characterized by a rather uniform cloud layer and cumulustratus clouds, which appear as large, darker somewhat cotton-like structures grouped in waves or lines. Cumulus, which are large and also consisting of cotton-like structures have their base in the low level, however often extending into the middle level. Likewise, cumulonimbus clouds have their base at the low level, and have a towering structure often reaching up to the high levels, sometimes expanding at the top giving it an anvil-like characteristic.

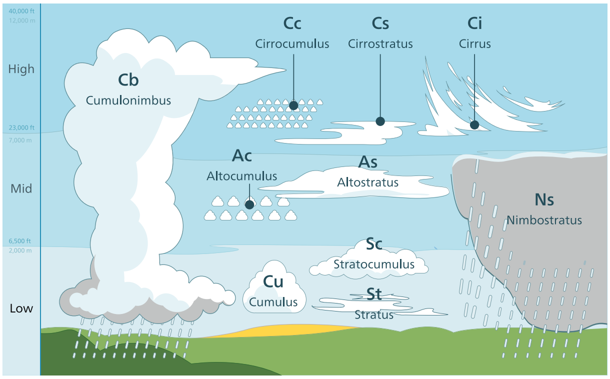

Figure 4: The ten genera of cloud types commonly associated with the troposphere. Author: Valentin de Bruyn. Licenced under Creative Commons CC-BY-SA 3.0 (https://creativecommons.org/licenses/by-sa/3.0/).

3.2 Cloud condensation nuclei

As mentioned in subsection 3.1, CCN are particles required for droplet and subsequently cloud formation to occur. CCN are a subset of the aerosol particles, either liquid or solid, present throughout the atmosphere which through their hygroscopic properties initiate droplet formation under the right meterological conditions. Mainly particle size, but also chemical composition govern the ability of a particle to act as a CCN and given a high enough supersaturation with respect to liquid water, virtually any aerosol particle would act as CCN. However, supersaturation with respect to liquid water in the atmosphere is most commonly found to be below 2 % and at these levels CCN ability is highly dependent on these particle properties. The atmospheric concentration of CCN will thus depend on both the variety of aerosol particles present as well as the local supersaturation levels, and these concentrations can vary between on the order of tens to thousands of CCN per cm^{-3}.

CCN originate from a wide range of different sources, such as marine and terrestrial ecosystems, volcanic emissions, biomass and fossil fuel combustion, which naturally varies depending on geographical region. The most abundant CCN are mainly composed of sea salt, sulfates or nitrates. Sea salt aerosols are mainly introduced to the atmosphere as sea spray via wind erosion and air bubbles bursting over the ocean surface, and these processes may also lead to the introduction of organic particles in biologically active ocean areas (Boucher et al., 2013). Nitrate aerosols are manly formed through atmospheric oxidation of NO_x gases, predominantly emitted from combustion processes. Biological emissions of sulfate precursor gases such as dimethylsulfate from phytoplankton also play an important role for atmospheric sulfate aerosol concentrations (Goto-Azuma et al., 2019).

The process of droplet growth and subsequent activation can be described by Köhler theory (Köhler, 1936), which is based on the particle physicochemical properties such as molecular weights, solute mass, number of dissociable ions, droplet size, density of water and solution surface tension. It combines the saturation water vapour pressure influence of water activity and the Kelvin effect on a droplet to describe the relationship between supersaturation and droplet size for droplet of these given properties. A convex liquid surface, such as a droplet surface, will give rise to a higher vapour pressure than that of a flat surface. This is described by the Kelvin effect, and is due to the fact that the molecules on a curved liquid surface has fewer possible neighbouring molecules to form a bond with and thus a higher probability of evaporating. Conversely, the opposite is true for a concave surface such as the inside of a bubble. The smaller these structures are, the larger the respective effects are.

Saturation water vapour pressure of the droplet is also affected by the amount and type of dissolved compound or compounds in the droplet solution. This is described by the water activity, which is the amount of water available for solvation of a solute. In Köhler theory this effect is accounted for with Raoult's law, which describes how the vapour pressure in the air above an ideal solution is depressed by an increasing solute concentration. From these concepts the Köhler equation is derived, which describes the relationship between supersaturation, droplet size and soluble particle material and mass for given an ideal solution.

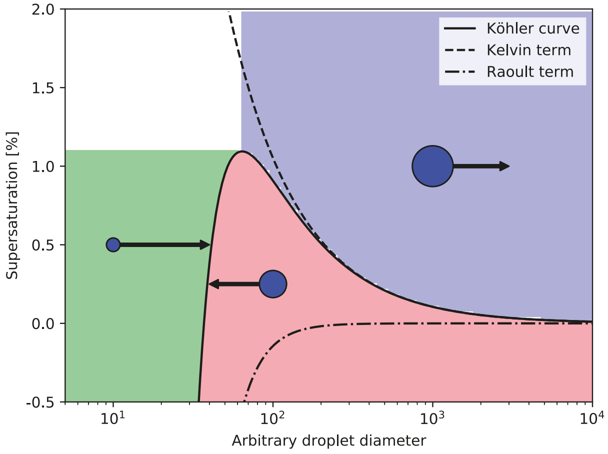

Figure 5: Köhler curve derived from Köhler theory, showing the water vapour pressure equilibrium (black line) with respect to supersaturation and droplet diameter for a given solute material and mass. In the red region, the droplets will evaporate and shrink due to water vapour pressure of the droplet being larger than the surrounding water vapor pressure. In the green region, droplets will grow, but only up until the equilibrium at the border with the red line. In the white area, a droplet might grow to activate given that the supersaturation does not decrease before it has grown large enough. In the blue area however, the droplets are free to grow indefinitely as long as they are subject to any degree of supersaturation. Also shown individually are the terms making up the Köhler equation (Equation 4); the Kelvin effect and Raoult's law.

The equation is shown in Box 3.1, and can be visually represented with a Köhler curve where supersaturation is plotted as a function of droplet size, which then represents the water vapour pressure equilibrium threshold for a given solute material and mass. Such a curve is shown in Figure 5 along with the individual Kelvin effect and Raoult's law components. Beneath this line, the supersaturation is too small to keep the droplet from evaporating and thus shrinking, however above line the droplets grow.

A droplet may grow for a given supersaturation, but this does not necessarily mean that it will be large enough to be able to grow further - activate into a *cloud droplet*. For this to happen, the droplet must reach a size where it can continue to grow indefinitely. This happens at the maxima of the Köhler curve, at which point the droplet is able to grow indefinitely. This is commonly called the critical supersaturation, and while a droplet may grow before this supersaturation is reached, its growth will halt at the equilibrium. As always, nature is a bit more complex than this, and the parameters and assumptions used by Köhler theory is not always enough to model and predict the CCN ability of certain aerosol particles. While inorganic compounds are very common in the atmosphere, low- to medium-hygroscopic organic compounds may also be present, and sometimes even dominate atmospheric aerosol mass concentrations (Kanakidou et al., 2005; Hodzic et al., 2020).

Aerosol particles may furthermore be internally and externally mixed, and are comprised of a range of different compounds either from primary emissions or through atmospheric ageing. Some mechanisms, such as uptake of soluble gases other than water vapour could even allow for stable droplets to exist under subsaturated conditions (Kulmala et al., 1997). Efforts have been made in the past to extend Köhler theory to give a better prediction as to how such more complex aerosol particles behave as CCN (Kulmala et al., 1997; Laaksonen et al., 1998). These modifications however, much like classical Köhler theory, still rely on knowing all properties of the included compounds which limits their application.

Box 3.1: Köhler Theory

The Köhler equation relates droplet size to supersaturation based on properties of a given initial solute, and is valid for droplets consisting of an ideal solution according to

$$S = a_w K \tag{1}$$

where S is the saturation ratio (where supersaturation s is given by $s = S - 1$, often presented as a percentage), a_w the water activity or Raoult's law term, and K the Kelvin term, defined as

$$K = \exp\left(\frac{4\gamma M_W}{\rho_W RTD}\right) \tag{2}$$

where γ is the solution surface tension, M_W the molar mass of water, ρ_W density of water, R the gas constant, T the temperature, and D droplet diameter. The a_w is not trivial and can be obtained in a number of ways, however is for practical reasons often approximated as

$$a_w = \left(1 + \frac{6 j_l m_s M_W}{M_s \rho_W \pi D^3}\right)^{-1} \tag{3}$$

where j_l is the number of dissociable ions, and m_s the mass of the solute. Note that a_w assumes a simple ideal solution. The Köhler equation is invalid for a large number of solutions, and to compensate for this j_l can be replaced by a correction factor accounting for the deviation from a non-ideal solution. One such factor is the van't Hoff factor which is often used as a constant over the whole range of solute concentrations. Taylor approximation then yields the commonly used form of Equation 1 as

$$S(D) = 1 - \frac{6 j_l m_s M_W}{M_s \rho_W \pi D^3} + \frac{4\gamma M_W}{\rho_W RTD} \tag{4}$$

where the second term represents the water activity/Raoult term a_w, and the third the Kelvin effect K. As can be seen, a_w and K are competing terms leading to the maxima and subsequent critical supersaturation in the Köhler curve, visible in Figure 5.

The hygroscopicity parameter κ has been introduced as a mean of providing a concise and readily comparable single-parameter value for the CCN ability of bulk aerosol particles. The concept was first introduced by Rissler (2005); Rissler et al. (2006), where it was defined as the number of soluble moles of ions or molecules per unit of dry particle volume. Petters and Kreidenweis (2007) independently proposed a conceptually similar hygroscopicity parameter, likewise named κ, which due to it's simplicity and applicability has become the most widely used parameterisation of aerosol particle CCN activity, and often referred to as κ-Köhler theory. From here on, κ will refer to the definitions of a dimensionless bulk hygroscopicity factor as made by Petters and Kreidenweis (2007), and a visualisation of this parameter can be seen in Figure 6.

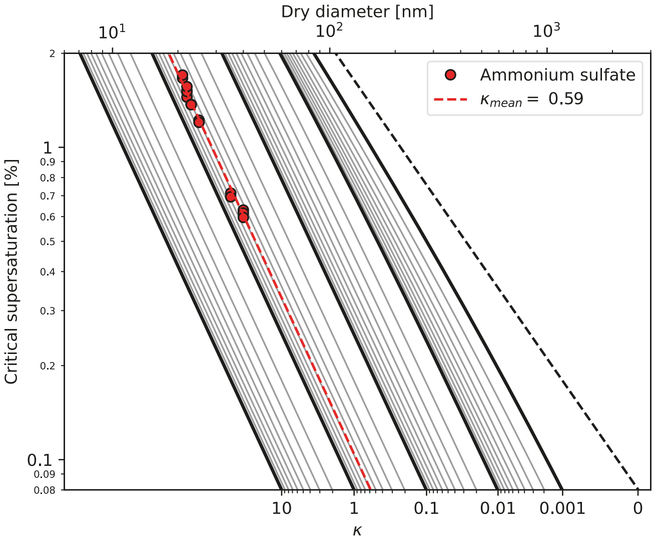

Figure 6: The κ values $0 \leq \kappa \leq 10$ shown in critical supersaturation - droplet size space. A $\kappa = 0$ represents non-hygroscopic particles, and for $0 \leq \kappa \leq 0.2$ a given κ is slightly curved, increasingly so toward $\kappa = 0$. This arises from the non-negligible contributions of dry particle to total water volume when equilibrium water content is relatively small. The most hygroscopic species found in the atmosphere have a κ of around 1.4. Ammonium sulfate measurements from this thesis work are included along with associated mean κ, based on calculations from Gysel et al. (2002). Visual representation of κ in critical supersaturation - droplet size space is adapted from Petters and Kreidenweis (2007).

κ-Köhler theory derives from Equation 1 of classical Köhler theory, and likewise defines supersaturation of a droplet size as being described by two competing physical phenomena; the Kelvin term and water activity. For κ-Köhler theory however, as can be seen in Box 3.2, the water activity is defined as depending solely on the fraction of dry particle volume to the water volume multiplied with the scalar κ parameter. Furthermore, the Kelvin term is approximated as to only relate to the properties of water, making the equation represent all particle physiochemical properties with the k. This enables κ values to be easily obtained with Equation 6 from measurements of particle populations without knowledge of their specific composition. This formulation has been reported to result in good agreement with model-based κ derived from Equation 5 for a variety of pure compounds, complex organic mixtures and ambient aerosol particles. However, larger disagreements has also been reported between modelled and measured κ, attributed to several effects not accounted for in Equation 6, such as highly non-ideal solution behaviour and surface tension effects (Petters and Kreidenweis, 2013). Surface activity has been reported to potentially significantly influence droplet growth (Prisle et al., 2010; Davies et al., 2019). There has been further developments of κ-Köhler theory of including a more detailed representation of the droplet solution influence on kappa by Petters and Kreidenweis (2013), however this formulation requires additional knowledge of the surfactant properties.

Box 3.2: κ-Köhler Theory

κ-Köhler theory (Petters and Kreidenweis, 2007) is derived from Equation 1, where the Raoult, or water activity term is redefined as the effect of the scalar hygroscopicity parameter κ on water activity as

$$\frac{1}{a_w} = 1 + \kappa \frac{V_d}{V_W} \tag{5}$$

where V_d is the dry particle volume, and V_W the droplet water volume. Based on the Zdanovskii, Stokes, and Robinson (ZSR) assumption for multiple solutes and water, i.e. that $V_w = \sum V_{wi}$, as well as the volumes can be expressed in their associated diameters as $D^3 = 6V/\pi$, together with Equation 1, 5 yields

$$S(D) = \frac{D^3 - D_d^3}{D^3 - D_d^3(1-\kappa)} K(D) \tag{6}$$

where S is saturation ratio (supersaturation s given by $S - 1$), D is the droplet diameter, D_d dry particle diameter, and K the Kelvin term described in Equation 2. This expression is the basis for κ-Köhler Theory.
The κ or critical supersaturation s_c is then obtained for a given D_d and either a known s_c or known κ respectively, either by finding the maximum of Equation 6 numerically, or from the approximate relationship valid for $\kappa > 0.2$,

$$\kappa = \frac{4A^3}{27D_d^3 ln^2(1+s_c)},\ A = \frac{4\gamma M_W}{\rho_W RT} \tag{7}$$

where γ is the solution surface tension, M_W the molar mass of water, ρ_W density of water, R the gas constant, T the temperature.

Petters and Kreidenweis (2007) hypothesised that the use of a constant surface tension $\gamma = 0.072\ J/m^2$ in the Kelvin term for all kappa approximations is beneficial, even though this may lead to over and underestimation of the κ parameter due to the difficulty in reliably predicting the surface tension of small droplets from bulk surface tension measurements as well as the unreliability of multicomponent mixture surface tensions (Topping et al., 2005). However, surface active compounds are known to be present in the atmosphere, and surface activity has been reported to significantly influence droplet growth (Prisle et al., 2010; Davies et al., 2019). This led to an extension of the original κ-Köhler theory seeking to account for such effects (Petters and Kreidenweis, 2013).

3.3 Ice nucleating particles

Although ice nucleation (IN) may appear conceptually similar to cloud droplet formation, the processes governing respective events are fundamentally different. Furthermore, in contrast to CCN the underlying processes are still poorly understood and there as of yet exist no established models able to explain, reproduce observations or provide parameterisations of the mechanisms behind ice nucleating particles (INPs) (Hoose and Möhler, 2012; Murray et al., 2012; Kanji et al., 2017; Knopf et al., 2018). As a result, computational modelling of cloud formation often apply homogeneous freezing for predicting IN (Fowler et al., 2020).

Primary ice crystals form homogeneously from water or pure solution droplets in the atmosphere at temperatures below about -38 °C. At subzero temperatures above this, droplets remain in the liquid phase as supercooled droplets unless heterogeneously formed by interacting with a solid surface able to lower the energy barrier and allow for the initial critical ice embryo to form. Such a surface can be provided by an INP, which may be able to facilitate IN of water directly from the gas-phase. At temperatures below -38 °C INPs may still be relevant for IN as long as the supersaturation with respect to ice is below approximately 40 % (Heymsfield et al., 2017).

Ice crystals play a significant role for cloud physical properties, as well as the chemical characteristics of the troposphere via for example adsorption of a wide range of atmospheric trace gases (Abbatt, 2003; Cantrell and Heymsfield, 2005). INPs are of importance to the properties of fully glaciated clouds in the cirrus temperature regime ($T \leqslant$ -38 °C) as well as fully glaciated, liquid or mixed-phase clouds (MPC) in the $0 > T >$ -38 °C temperature regime. Over land areas, precipitation is predominantly due from glaciated clouds (Mülmenstädt et al., 2015).

Because MPCs are ubiquitous to the troposphere, they have a central role both regionally and globally in the precipitation and life-cycle of clouds (Korolev et al., 2017). MPCs are clouds that consist of both ice crystals and supercooled liquid droplets, and the presence of ice crystals asserts a heavy influence over the clouds supercooled liquid water content through what is called the Wegener–Bergeron–Findeisen (WBF) process. Since the saturation water vapour pressure with respect to ice is lower than the saturation water vapour pressure with respect to liquid water, ice crystals will when the ambient water vapour pressure lies between the two start to grow to precipitation sizes at relatively short time scales at the expense of the liquid droplets. In other words, relatively few ice crystals will grow at the expense of many droplets, changing the clouds reflective properties and increasing the likelihood of precipitation. Consequently, although INP concentrations are on average very low in the troposphere, at around one INP per 100,000, they can assert a disproportionate influence on clouds (DeMott et al., 2010).

Heterogeneous IN stems from the single phenomenon of a surface lowering the energy barrier for a critical ice embryo to form from either supercooled liquid or gas-phase water. This can happen via different pathways, commonly referred to as modes and categorised into the following four: immersion freezing, contact freezing, deposition freezing, and condensation freezing. The terminology below is largely based on the one put forward by Vali et al. (2015).

Immersion freezing is where heterogeneous IN is initiated from an INP immersed in a supercooled liquid droplet. The introduction of the INP into the droplet may arise from different scenarios, such as collision of an INP with an existing droplet in conditions unfavorable for INP activation. However, it is more likely to stem from CCN activation of the same particle. For example, an INP active particle core with a soluble CCN active coating would after droplet formation expose the core and lead to IN of the droplet. Immersion freezing is believed to be a dominant pathway of IN in higher temperature conditions, and in particular for mixed-phase clouds (MPCs) (de Boer et al., 2011; Hande and Hoose, 2017; Knopf et al., 2018).

Contact freezing occurs when the surface of an INP comes into contact with the air-liquid interface of a supercooled droplet either from the outside via collision, or from the inside via droplet evaporation and has been observed to occur at higher temperatures than immersion freezing (Durant, 2005). Niehaus and Cantrell (2015) found contact freezing to occur when different solution droplets collided with supercooled water droplets, indicating IN initiated via impact. However, the study was limited to large particles (25 - 150 μm), and so the phenomenon has not been observed for smaller sizes, limiting the relevance for atmospheric cloud droplets and INP. Nagare et al. (2016) compared IN from both immersion and contact freezing reported similar activity for both modes, putting into question the relevance of the actual contact event as relevant for IN under atmospheric conditions.

Deposition freezing is a heterogeneous IN process in which gas-phase water deposits directly on to a solid surface. It is the only IN process in which water vapour enters the ice-phase without first entering the liquid phase, and occurring where there is ambient supersaturation of water vapour with respect to ice but not liquid. However, it has recently been shown that liquid water may exist in subsaturated conditions with respect to liquid water in small concave geometries, or pores of a solid particle due to the inverse Kelvin effect, which subsequently freezes (Marcolli, 2014; Campbell and Christenson, 2018; David et al., 2019). This phenomenon has given rise to the term pore condensation freezing, and previously reported deposition IN activity may instead have been due to pore condensation freezing (Marcolli, 2014). IN from deposition and pore condensation freezing are expected to be of most relevance to cirrus clouds (David et al., 2020).

Condensation freezing is conceptually closely linked to immersion freezing and deposition freezing. It is the heterogeneous IN process in which water vapour condensation and freezing occur concurrently at supersaturated conditions. However, it is not clear if condensation freezing is truly a separate process from either immersion freezing or deposition freezing (Vali et al., 2015).

Ice crystals formed from secondary processes are also likely to be a significant source of ice crystals in the troposphere. These secondary ice crystals form when an ice crystal to some degree fragment as a result of different mechanisms. Most proposed mechanisms are tied to the freezing event of a droplet, such as isolated pockets of liquid in an otherwise frozen droplet causing the droplet to shatter when said pocket freezes and expands, or when an ice crystal is subjected from thermal shock due to interacting with a supercooled droplet (Korolev and Leisner, 2020). However, it is still largely unknown what mechanisms are dominating this effect in the troposphere.

3.4 Soot as ice nucleating particles

The role of soot containing particles in atmospheric IN is inconclusive. While previous studies have shown soot to be relevant for IN in the cirrus temperature regime of T $\leqslant$ -38 °C (Möhler, 2005; Koehler et al., 2009; Kanji et al., 2011; Hoose and Möhler, 2012; Kulkarni et al., 2016; Ullrich et al., 2017), the role these particles play in the MPC regime of T $>$ -38 °C is unknown. It is of special interest in the scientific community owing to the large natural and anthropogenic regional and global emission rates and thus its potential to influence cloud properties, especially MPCs. However, the vast literature of laboratory and field studies on soot IN ability has remained contradictory (Bond et al., 2013; Kanji et al., 2017). As described in subsection 2.1, soot particles has very complex and varying physicochemical characteristics dependent on combustion conditions and post-combustion atmospheric processes which may lead to properties relevant for IN.

Several studies have previously reported soot particles to activate IN via immersion freezing in temperature ranges relevant for MPCs. DeMott (1990) reported soot particles from an acetylene burner to initiate immersion mode ice nucleation up to T = -24 °C depending on INP size, and approached an activated fraction of 3 % at T = -35 °C, thus of relevance to MPCs. Experiments with Lampblack commercial soot have likewise suggested positive results on immersion mode IN (DeMott et al., 1999; Dymarska et al., 2006; Brooks et al., 2014). Although the study of Dymarska et al. (2006) was mainly focused on deposition mode IN, the experiments observed immersion IN at T $\geq$ -25 °C, thus relevant to the MPC temperature regime. The study reported no IN enhancement from ozone oxidation of the soot. Brooks et al. (2014) reported mean freezing temperatures of -24 to -19 °C, and in contrast to Dymarska et al. (2006) observed a consistently enhanced effect from ozone oxidation prior to freezing, potentially due to the differences in primary particle sizes between the studies. DeMott et al. (1999) only studied immersion IN at T $\leq$ -40 °C. Other studies have found soot to have little to no immersion IN activity. Friedman et al. (2011) tested the immersion IN ability of soot generated with a miniCAST (see section 4.1), coated with a variety of acids, and Chou et al. (2013) in experiments with fresh and aged diesel soot particles, but neither detected any immersion IN activity in the MPC temperature regime.

More recent studies have more seriously questioned the relevance of soot in the MPC temperature regime (Vergara-Temprado et al., 2018; Mahrt et al., 2018; Kanji et al., 2020). Vergara-Temprado et al. (2018) performed laboratory tests on immersion IN activity with a cold stage (see section 4.3), on soot particles generated with a burner from *n*-decane and eugenol fuels and found no detectable IN activity beyond uncertainty. Furthermore, they reported that previously reported estimates of soot n_s (Murray et al., 2012), based on earlier measurements (DeMott, 1990; Diehl and Mitra, 1998), might be overestimated by more than two orders of magnitude. Kanji et al. (2020) performed studies on several types generated soot in different sizes: regal black, fullerene-enriched soot from nebulisation, mature and partially matured soot from a miniCAST, as well as soot from a spark generator. The study reported little to no immersion IN in the MPC regime, and additionally performed a short review of previous laboratory measurements prompting the study to conclude more broadly that soot particles are not relevant for the MPC temperature regime.

While it is certainly possible that fossil fuel-derived soot particles are near-irrelevant for immersion IN as discussed above, the knowledge gap as to the underlying properties governing observed IN activity in the MPC temperature regime is however still tremendous. Even only small subsets of more IN active soot particles could potentially dominate INP concentrations in some regions, depending on seasonal variation of other INPs, illustrating the need to know more about soot IN mechanisms. A recent study by Jahn et al. (2020) reported that mineralisation of inorganic elements in the biomass combustion led to soot particles containing IN active mineral sites, which induced immersion freezing for temperatures up to -13 °C. Atmospheric processing has furthermore been reported to enhance the IN activity of such particles (Jahl et al., 2021). This development, while not explicitly tied to soot particles, could potentially aid in better understanding the implications of biomass combustion emissions on INP concentrations.

4 Methodology

4.1 Soot sources

miniCAST flame soot generator

For paper I & II, soot particles were generated with a miniature combustion aerosol standard soot generator (miniCAST, model 5201C; Jing ltd.) to study soot ice nucleation and physicochemical properties. A schematic over the principle of operation can be seen in Figure 7. The miniCAST generates particles from the controlled burning of a propane co-flow diffusion flame located inside the instrument. The combustion conditions for the flame and consequently also soot particle properties can be controlled via four gas flow parameters: 1) propane fuel at the center of the burner, 2) N_2 for pre-combustion fuel mixing, 3) N_2 for flame quenching at a set height above the fuel outlet, and 4) air oxidation at the perimiter of the flame. The miniCAST also provides an air flow parameter for dilution of particle emissions. In the experiments we controlled these flow parameters in two different ways to produce particles with different levels of soot maturity and chemical composition: 1) by modifying air oxidation flow, and 2) by modifying air oxidation flow and N_2 pre-combustion mixing flow.

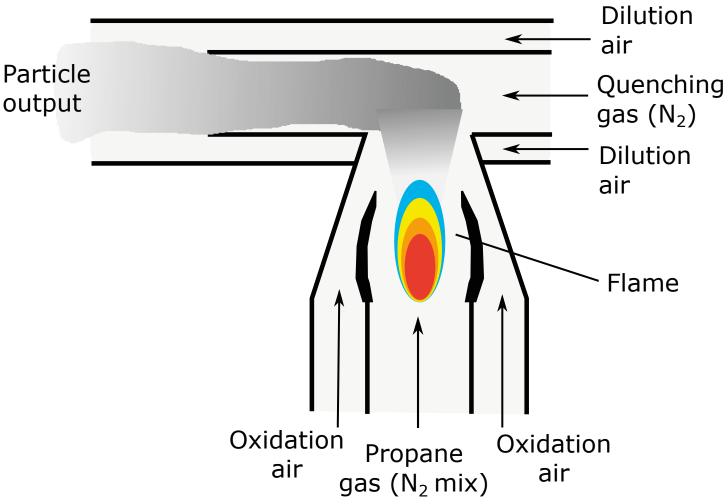

Figure 7: Operating principle of the miniCAST. Propane gas is supplied at the bottom, potentially mixed with N_2 gas. Oxidation air is supplied on the perimeter of the flame. A constant N_2 quench gas flow is provided at a set height above the flame, and the emissions can be further diluted with the dilution flow. All flows except the quench gas flow are adjustable.

Heavy-duty diesel engine

In paper III, diesel engine emissions were produced with a six-cylinder in-line Scania D13 heavy-duty diesel engine modified for single-cylinder operation. Engine emission output was studied both directly, as well as after having gone through a combination of emissions after-treatment systems: a diesel oxidation catalyst (DOC), and/or a diesel particulate filter (DPF). Three types of fuels were tested: one fossil fuel (EN 590 compliant 150 ultra-low sulfur fossil diesel), and two renewable diesel fuels (hydro-treated vegetable oil, and rapeseed methyl ester). All three fuels were investigated without any blending. The various emissions were measured for three combinations: 1) engine-out (no after-treatment), 2) DOC only, and 3) DOC and DPF. However, since DPF was found to remove nearly all particles relevant to IN activity, it was not included in the study. The resulting sample aerosol was diluted via both a porous tube diluter (PTD), and an ejector diluter (ED) to achieve atmospherically relevant concentrations. Additional experiments were performed by subjecting the sample aerosol to 1) photochemical ageing with an oxidation flow reactor, and 2) photochemical ageing as well as removal of volatile species particle matter with a thermodenuder. When used these were located between the PTD and the ED.

Biomass cook stoves

The cook stoves which were studied in paper IV and V were part of the Salutary Umeå STudy of Aerosols IN biomass cookstove Emissions (SUSTAINE) campaign performed at Umeå University, Sweden during 2016. This study sought to characterize the health and climate impact aspects of cook stoves relevant to the sub-Saharan Africa region. The study included four types of cook stoves representing different technological levels: three-stone fire, rocket stove, natural draft gasifier stove, and forced draft gasifier stove. Seven different solid fuels in either wood log or pellet form were used, and a summary can be seen in Table 1.

The three-stone fire is the most widely used type of cook stove for every-day heating, cooking and lighting in the least developed regions of the world. As the name suggests, its is basically an open fire surrounded by (three) stones or bricks. The rocket stove is a more advanced type of stove, consisting of a bottom-fed vertical cylindrical combustion chamber with an insulating outer shell. The resulting natural draft from the bottom causes a more efficient combustion of the fuel.

Gasifier stoves have in similarity to the rocket stove and up-right cylindrical design. They are based on the principle of a two-stage combustion process, where heat in a pyrolisation process volatilises combustion gases from the pellet fuel bed at the center bottom of the stove under which the primary air supply is located. A secondary air supply is found near the top of the stove, and when the volatile gases are mixed with the secondary air supply a hot flame is created. The difference between a natural and a forced draft stove is that in the forced draft stove the primary and secondary air supply ratio is actively controlled via an electrical fan.

The experiments were performed by conducting a modified standard water boiling test, in summary consisting of boiling a 5L volume of water with an initial temperature of 20 °C for 45 minutes. The combustion exhaust was sampled with an extraction hood at dilution rates of 1:20 to 1:50, and sent into a 15 m^2 chamber after further dilution.

Table 1: Overview of the fuels and fuel mixtures studied in papers IV & V.

Fuel	Form	Comments
Sesbania sesban	Wood logs, pellets	-
Casuarina equisetifolia	Wood logs, pellets	-
Coffe husk	Pellets	50/50 % Softwood
Rice husk	Pellets	50/50 % Softwood
Water hyacinth	Pellets	50/50 % Softwood
Swedish birch	Wood logs	-
Softwood	Pellets	Commercially produced pine and spruce mixture

4.2 Cloud condensation nuclei measurements

For paper V, a Cloud Condensation Nuclei counter (CCNc; model CCN-100; Droplet Measurement Technologies) was used to measure CCN activity of combustion particles. The CCNc operates on the principle that the diffusion of water vapour in air is faster than the diffusion of heat in air, and a conceptual schematic can be seen in Figure 8. The instrument is made up of a 0.5 m long cylindrical column, with walls consisting of a porous material continuously wetted with water supplied from the top of the column. The sample flow is located along the center of the column, surrounded by a sheath flow. A temperature gradient is established along the column via a number of peltier elements, with increasing temperature along the aerosol flow. Given that the water vapour is saturated along the whole column wall, water vapour partial pressure is lower at point A than point B. Since the partial vapour pressure is equal at point B and C, but the temperature in point C is lower than point B from the diffusion of heat being slower than the diffusion of water vapour, point C contains more water vapour than what at the lower temperature would be considered saturated - thus causing supersaturation at that point. The level of supersaturation is dependent on the temperature difference at point A and B, and thus changing this gradient also changes the supersaturation at point C.

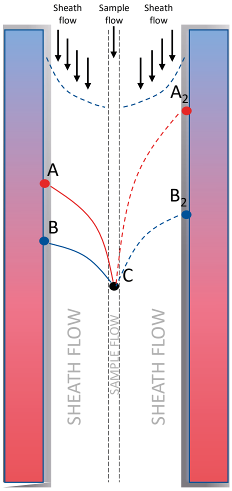

Figure 8: Operating principle for the CCNC. The column walls have an increasing temperature going from the top towards the bottom, denoted as a blue-red gradient. The sample flow carrying the aerosol particles goes through the center axis of the column, surrounded by a sheath flow of clean air. The red lines represent diffusion of heat, and blue lines diffusion of vapour. The points A and B represent points along the column wall, with different temperatures but both at saturated water vapour conditions, causing a constant supersaturation along the sample flow region for a given temperature gradient and total flow. Point A_2 and B_2 with dashed lines show the increased temperature difference between the points when the temperature gradient is kept the same as for A and B, but total flow instead is increased. This is the principle behind the scanning flow method of varying supersaturation.

The temperature gradient takes on the order of minutes to stabilise after having been changed, and so the original method of operating the CCNc is by performing longer measurements at a constant supersaturation, for a few selected values. However, a similar effect to changing the temperature gradient can be achieved from varying the total flow through the CCNc column (Moore and Nenes, 2009). Again, due to the difference in diffusion of heat versus water vapour a higher flow lead to a smaller distance for both point A and B to point C and thus a smaller temperature difference, and vice versa.

In paper v, the scanning flow method was used for all CCN activity measurements, varying the total flow between 0.2 and 1.0 Lmin^{-1} over 120 s. To compensate for the variation in flow otherwise seen by the rest of the experiment setup system, a bypass flow controlled with a mass flow controller was kept in parallel with the CCNc to keep the flow rate at a constant 1.0 Lmin^{-1}. The CCNc was always used in series with a Differential Mobility Analyser (DMA Model 3081, TSI Inc., USA) to study quasi-monodisperse particle populations.

4.3 Ice nucleating particles measurements

In the papers performing ice nucleation measurements, two different methods were used for measuring immersion freezing ice nucleation. In Paper i, iii and iv, a Continuous Flow Diffusion Chamber (CFDC) was used for examining ice nucleation properties of aerosol particles in real-time by exposing an aerosol particle sample flow to controlled RH and temperature conditions. In paper II, a droplet-on-substrate cold stage based method was used for analysis of aerosol particle immersion ice nucleation activity, described in section 4.3.

Continuous Flow Diffusion Chamber

The SPectrometer for Ice Nucleation (SPIN) is a CFDC used for examining ice nucleation properties of aerosol particles in real-time by exposing an aerosol particle sample flow to controlled RH and temperature conditions. The instrument consists of two chambers; a main chamber and an evaporation chamber. The main chamber is made up of two parallel 1.0 m long and 0.3 m wide aluminium plates separated by 1.0 cm. Sixteen thermocouple pairs are situated along the length of the plates, although in the studies only the uppermost 13 were used for measuring the temperature as they represent the main chamber conditions (Garimella et al., 2016). A sample flow of 1.0 Lmin^{-1} surrounded by two sheath flows of 4.5 Lmin^{-1} each run between the plates along the length of the chamber. The two plates are each cooled down to a different sub-zero temperature and coated with a thin layer of ice, typically around 1 mm. The difference in temperature between the two plates lead to heat and water vapour diffusing from the warmer wall towards the colder, and the non-linear relationship between saturation vapour pressure and temperature leads to supersaturation with respect to ice. A high enough temperature difference between the plates results in water vapour partial pressure in the sample flow region to also exceed the saturation vapour pressure for liquid water. This is needed in order to study immersion ice nucleation, and in the experiments we used SPIN with a supersaturation of approximately 10 % with respect to liquid water.

The evaporation chamber is as the name suggests used to evaporate droplets that were not activated to form ice in the main chamber. This is achieved by having the evaporation chamber walls at isothermal conditions, which causes sub-saturated conditions for liquid water but not for ice. The SPIN evaporation chamber is small compared to other similar CFDCs and droplets may co-exist with ice crystals under a larger range of operating conditions. The resulting particles are in the SPIN detected with an size-resolved Optical Particle Counter, which additionally records particle polarisation data. This data can be used to filter liquid particles from the measurement data if needed.

The version of SPIN which were used in this study could not reliably discern detected particle phases, and thus data analysis used the concentrations of particle diameter $\geq 6\ \mu$m as a criteria for having detected ice crystals. In experiments, the temperature was scanned in low-to-high and high-to-low ramps which lasted about 11 minutes each, however due to better temperature control only low-to-high data was used for analysis. Typical temperature range scanned was -41 to -32 °C. A Differential Mobility Analyser (DMA Model 3081, TSI

Inc., USA) was used in most measurements to pre-select quasi-monodisperse distributions. In paper IV, the SPIN was for some experiments also run by keeping a constant temperature in the sample flow region, and varies the relative humidity with respect to ice, which since both are dependent on the temperature gradient also varies relative humidity with respect to water.

Cold Stage

For paper II, immersion ice nucleation was analysed by cold stage measurements on the Lund University Cold Stage (LUCS) setup. The basic principle is to collect aerosol particulate matter, and later transfer it into a batch of clean water. Droplets from this sample water is then placed in a small cold stage (model LTS120, Linkham Scientific) chamber in which the temperature is lowered at a constant rate and droplet ice activity recorded. This activity is recorded with a camera (Canon Eos 6D mk II, Canon, JP) taking images at constant intervals through a window in the enclosed cold stage.

In the experiments soot particles from each experiment were collected on nucleopore filters. Since only a fraction of the soot particles on these filters are transferred to the water, as much particulate matter as possible was collected on the filters. After filter collection the water samples were prepared in a ultra-clean environment with 0 particles cm^{-3} by taking half of the filters and placing them in an analytical grade vial, and adding 2 mL of 18.2 MΩcm Milli-Q water. The cold stage is prepared by placing four hydrophobic silicon-treated glass slides next to each other on the cooling element in the cold stage, and on top of them a silicone grid sheet containing 100 hexagonal holes, see Figure 9.

The sample water was distributed in 1 μL drops in each of the 100 grid holes, and an acrylic glass slide additionally placed above the silicone grid sheet to create a sealed environment for each droplet, however only being in contact with the silicon glass slide beneath. The cold stage temperature was lowered to -5 °C before the actual measurements start, to save time and assure that no condensation appeared between the cooling element and the silicon glass slides. The cooling is provided by a thermoelectric element, with its heat sink kept at a constant temperature by circulating cold water from a reservoir of through it. A measurement series then consisted of gradually lowering the cold stage temperature at a rate of 2 $^{\circ}Cmin^{-1}$ while images of the droplets as well as the corresponding cold stage temperature is recorded at 5 s intervals until all droplets have been observed frozen. Equivalent measurements with pure Milli-Q droplets are regularly preformed as a calibration for the background. Analysis consists of either manually or automatically going through the image and temperature data and tie the accumulated frozen fraction of droplets to the corresponding temperature.

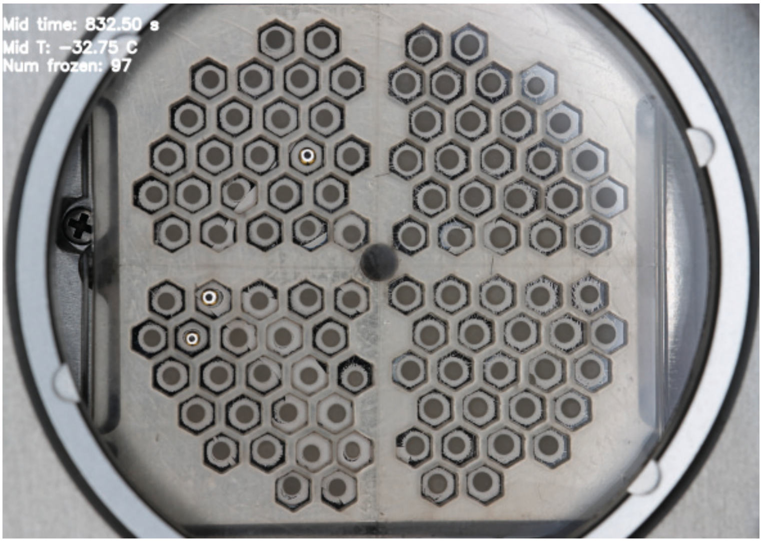

Figure 9: The Lund University Cold Stage chamber. Depicted is the chamber used to measure immersion IN activity by cooling down 1 μL droplets in sets of 100, placed on hydrophobic silicon-treated glass slides in a silicone grid. The activity is recorded at 5 s intervals with a camera along with corresponding temperature.

The images were automatically analyzed using custom-made software. The software initially uses image processing and analysis to determine the square regions of interest (ROI) of each droplet. After this, the software analyses each image for each ROI, and establishes an associated phase score. The phase score is based on the saturation value of the ROI image converted to the HSV color space, which provides a clear signal to when the ice has started to form in the droplet. This method is dependent on the light and camera setup of the LUCS, however provides a fast and convenient way of processing several experiments. Summary images of all adjacent ROI images of a freezing event are generated and reviewed before a result is accepted. Each freezing event is linked to the associated temperature of each image, and from this it an activated fraction as a function of temperature can be derived.

5 Thesis findings

5.1 Challenges in linking physicochemical properties to soot IN activity (I & II)

Paper I & II examined the possibility of finding correlations between IN activity of freshly emitted soot particles and a range of their ensemble physicochemical properties. In paper I, eight different soot particle types of varying soot maturity were generated with a miniCAST flame soot generator, representing a wide range of physicochemical properties. Out of the eight samples only one exhibited immersion IN activity patterns clearly distinguishable from homogeneous freezing, while an additional three out of the eight samples showed slight immersion IN activity. No significant correlations could be found for any of the included parameters, though for a subset containing partially matured soot indications on an enhancement of IN activity from increasing levels of PAHs and effective density was observed, see Figure 10. When extending the dataset to include results from paper III, no correlations could be seen, and furthermore the most ice active sample from that study did not show any elevated levels of PAHs or effective density. The results indicate that the properties governing IN activity might only be present in sub-populations of the observed sample particles, and that it might not be feasible to use on-line ensemble measurement methods for identifying IN relevant characteristics with soot particles.

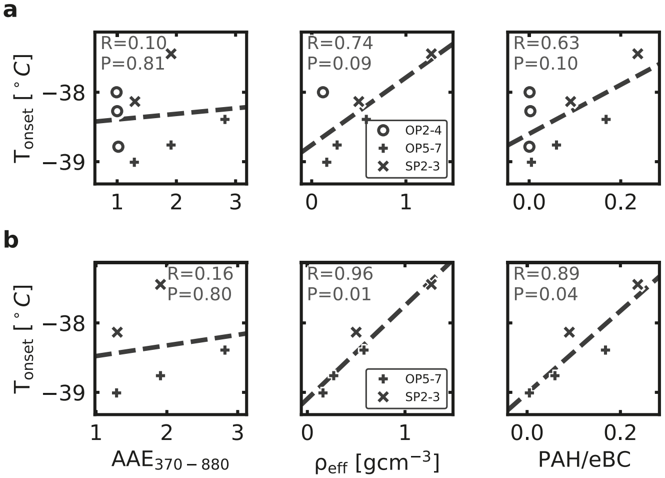

Figure 10: Results from paper I. Pearson correlations for the physicochemical parameters from paper I which showed the largest correlations for: (a) All samples from the study, and (b) a subset of the partially matured samples.

Paper II was a continuation of the research questions of paper I, and sought to evaluate the physicochemical properties and immersion IN activity of aged and thermally treated soot particles from a miniCAST flame soot generator. The study focused on a smaller set of two different partially matured soot particle types, for four different particle treatment configurations. An oxidation flow reactor (OFR) was used to simulate atmospheric ageing at high and low UV intensities, and a thermodenuder (TD) was used to alternatively remove volatile species from the particles. The particle types were tested for the following configurations: 1) No treatment, 2) OFR, 3) OFR followed by TD, and 4) TD followed by OFR. The sample physicochemical properties were measured with on-line instrumentation, however unlike paper i the immersion IN activity was measured from filter samples using the off-line LUCS cold stage instrument.

The studied samples saw a generally low immersion IN activity, and only five of the twelve samples activated at around 1 K above the background. The immersion IN activity was analysed based on estimated ice active sites per unit surface area of soot. There was a trend of decreasing IN activity for higher UV intensities in otherwise identical configurations, as well as a depression of IN activity from using only the OFR compared to no treatment. As in paper i, no noticeable correlations between physicochemical properties and immersion IN activity were found over the whole dataset. It was observed however, that several samples from different treatment configurations had very similar physicochemical properties for all studied properties, yet exhibited noticeable differences in immersion IN activity. These observations further supports the hypothesis from paper i, that only a subset of the particles are responsible for observed IN activity, and on-line ensemble methods might thus not be able to capture the properties governing the observed immersion IN activity.

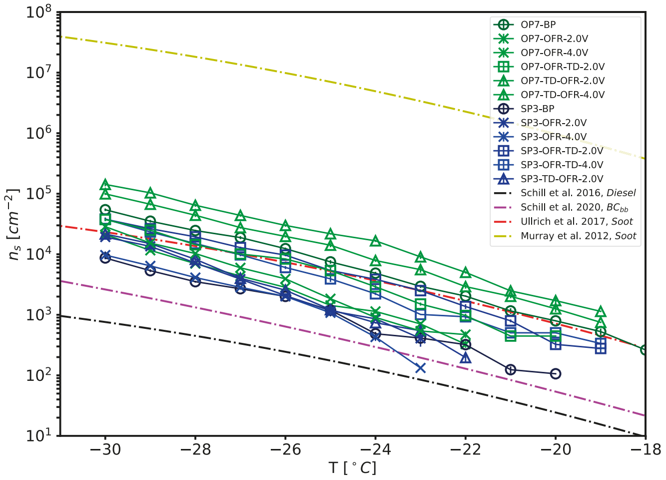

Figure 11: Results from paper ii on ice nucleation efficiency expressed as estimated ice active sites per unit area of soot (n_s) for two different miniCAST settings (denoted OP7 and SP3) and the four treatment configurations. PAM stands for Potential Aerosol Mass, and is a type of oxidation flow reactor, and the number for each sample when present represents UV intensities. Included in the figure are also four soot parameterisations from the literature. BC_{bb} denotes parameterisation of biomass burning particles.

5.2 IN activity of Diesel and cook stove combustion emissions (III & IV)

Paper III & IV investigated the immersion ice nucleation activity of emissions from two types of real-life related sources in a laboratory context. In both papers, a key aspect was the immersion IN activity of combustion emissions from renewable fuels.

Paper III performed studies on the combustion emissions from a heavy-duty diesel engine with three different fuels. Two renewable; hydrotreated vegetable oil (HVO) and rapeseed methyl ester (RME), as well as one fossil; low-sulfur diesel fuel were studied. The combustion emissions were also studied after having passed through different aftertreatment systems. The fuels were used without any blending to enable observations of the isolated properties of each fuel. The fuels were additionally photochemically aged with an OFR to simulate atmospheric processing. The results showed an over all low immersion IN ability for all studied fuels and aftertreatment combinations. For the experiments with photochemical ageing, only fossil fuel diesel saw a discernible albeit small increase in IN activity. All of the experiments exhibited a low CCN activity at high supersaturation conditions with respect to liquid water, which gives an underestimation of the IN activity. However, performing corrections for this is not trivial, and while a simplified correction did shift immersion IN activity slightly into mixed-phase cloud relevant temperatures as seen for HVO in Figure 12, no reliable conclusions can be made from this. The overall results of paper III add to the growing set of studies identifying both fresh and aged diesel combustion particulate emissions as poor INPs (Chou et al., 2013; Schill et al., 2016).

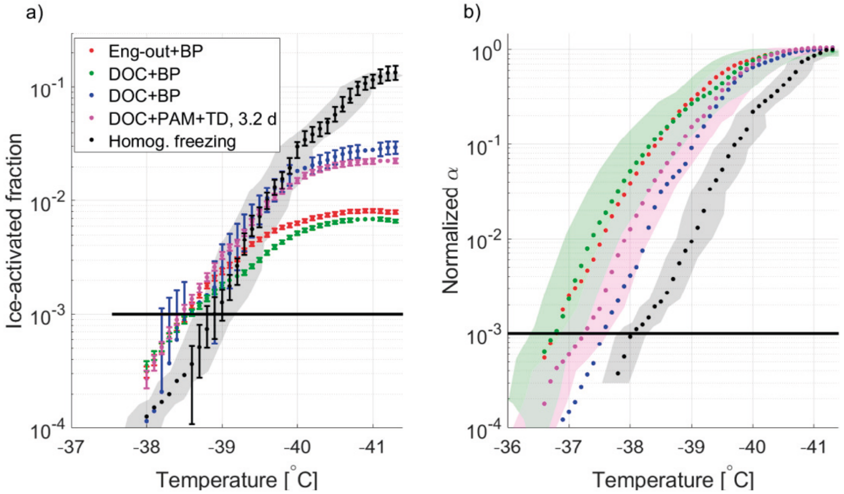

Figure 12: Results from paper III on emissions from a heavy-duty diesel engine burning hydrotreated vegetable oil (HVO). Original caption: Ice-activation spectra of HVO emissions at RH_{water} = 110 %, compared to homogeneous freezing test of droplets. The shaded areas of respective colors represent the T-span on the lamina during the experiments. The error bars represent the random error from detectors (two standard deviations), and the shaded areas of respective colors represent the T-span on the lamina during the experiments. The solid black line indicates 0.1 % activated fraction. Panel a) presents the ice-activation of whole sample population polydisperse aerosol), and panel b) a situation where all activation spectra are normalized to the highest ice-activation fraction fromeach respective experiment. "Eng-out" refers to a case without emission aftertreatment, and BP = bypass (sample treatment method).

In paper IV, measurements on deposition and immersion IN activity were performed with the SPIN as part of the larger SUSTAINE campaign which studied combustion emissions from a range of cook stoves and biomass fuels in majority related to sub-Saharan Africa (described in more detail in section 4.1). Paper IV performed cook stove particle emission measurements on both transient polydisperse populations, and mobility size-selected quasi-monodisperse populations from a $15 m^{-3}$ aerosol-storage chamber. The study found no detectable deposition or immersion IN activity from transient measurements of fresh polydisperse combustion emissions at constant T = -28 or -32 °C and varying RH_{water} between ~75 - 105 %, however we noted that the particle distributions contained large number concentrations of ultrafine particles, possibly obscuring the results by passing through the SPIN undetected. The chamber measurements looked at the immersion IN activity of accumulation mode particles in the range of 250 - 500 nm mobility-equivalent diameters, for temperatures between -43 and -32 °C at a constant RH_{water} of 115 %. In those experiments, all cook stove and fuel combinations studied, except two, showed moderate but obvious immersion IN activity above homogeneous IN temperature, generally about 1 - 1.5 °C. The study also performed five additional measurements where combustion conditions were modified to lower the combustion efficiency, in which immersion mode IN activity was as high as 5.9 °C above homogeneous IN temperature (Figure 13). It should be noted that all particles studied were from relatively fresh emissions, and that atmospheric ageing might influence the particle IN activity.

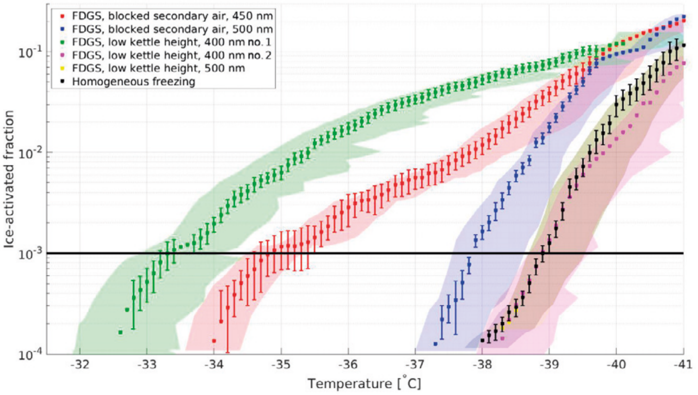

Figure 13: Results from paper iv, where softwood pellets (SW) were burned in a forced-draft gasifier stove (FDGS) under modified conditions that induced inefficient combustion conditions in two ways: 1) by blocking the secondary air inlet, and 2) changing the kettle height causing larger particles to be produced.
Original caption: Ice-activation spectra of emissions from combustion of SW pellets in forced-draft gasifier stove, with modified combustion conditions at RH_w = 115 %. Each shaded area of respective color represents the T span across the lamina (maximum uncertainty) during each observation. The error bars present combined relative standard deviations in particle detection by the CPC and OPC of the SPIN. The solid black line presents the 10^3 activation threshold. The ice-activation spectrum for homogeneous freezing is included for comparison.

5.3 High variability in CCN activity of cook stove combustion emissions (v)

Paper v was, as paper iv, part of the SUSTAINE campaign, and studied the CCN activity aspect of combustion particle emissions for four types of cook stoves and seven types of biomass fuels primarily related to sub-Saharan Africa conditions (see section 4.1). CCN activity κ (see subsection 3.2) from combustion particle emissions was determined with a CCNc from quasi-monodisperse populations of a given size in the range of about 65 to 350 nm based on mobility-equivalent diameter. Like in most of the measurements of paper iv, the particles were collected in a 15m^{-3} chamber prior to measurement.

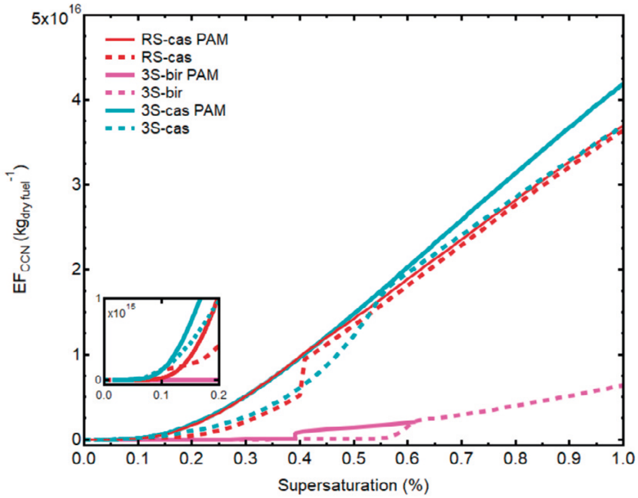

Figure 14: Results from paper v, comparing freshly emitted and aged emissions from a subset of stove-fuel combinations: Rocket stove an casuarina logs (RS-cas); Three-stone stove and casuarina logs (3S-cas); and three-stone stove with birch logs (3S-bir).
Original caption: Examples of emission factors of CCN as estimated for the aerosol photochemically aged inside PAM with the fresh emission factors included for comparison. For the 3S-cas PAM experiment, the nucleation particle mode grew large enough to dominate near a mobility diameter of 65 nm, which resulted in an increase in CCN for high supersaturations.

The CCN activity of the studied samples observed a large variation depending on both cook stove and fuel type, and the study noted higher κ for more advanced stove technologies. κ was also seen to decrease along with effective density for increasing particle sizes. The study derived estimates of primary CCN emission factors (EF) for each sample based on κ and measured particle number distibutions. These CCN EFs likewise exhibited large variations between samples, in large part due to the variations between particle number distributions and mostly associated with the use of different fuels. It could furthermore be observed that higher concentrations of potassium in the dry fuel had a strong impact on CCN EFs. The study additionally compared CCN EFs of fresh emissions samples with photochemically aged of the same stove-fuel combinations (Figure 14). The photochemical ageing was seen to increase CCN concentrations for low supersaturations, and potentially also for high supersaturations of around 0.6 - 1.0 % due to new particle formation and growth. The results of paper v show that biomass-fueled cook stoves may be a significant source of CCN, and changes in this source due to shifts in either stove or fuel use could have warming implications on the climate.

6 Conclusions & outlook

The research presented in this thesis has sought to provide more insight into some of the many uncertainties that yet exist regarding the role of combustion particles, and especially soot, in atmospheric cloud processes. Specifically, through laboratory studies, the research has been aimed at characterising soot particle properties in an effort to relate these to their IN activity, as well as investigating IN and CCN activity of renewable fuel combustion sources linked to real-life anthropogenic activity.

The laboratory studies we performed on soot particles from a flame soot generator showed an overall low to insignificant immersion IN activity of freshly produced and photochemically aged, partially matured to mature soot. Our efforts in trying to identify links between immersion IN activity and soot physicochemical properties were generally inconclusive, and no significant correlations could be found in the data from neither paper I nor II. We did in paper I observe indications that increased levels of organics and PAHs enhanced IN activity for a subset of partially matured soot particles, however as such correlations did not persist between studies we judge it unlikely to be a reliable observation. In paper II we did observe different configurations of photochemical ageing in combination with thermal treatment to have an effect on immersion IN activity of partially matured soot. Several of these configurations exhibited to a large degree similar soot particle phyicochemical properties, and at the same time a considerable difference in immersion IN activity. The results of these studies indicate that the properties governing IN activity are not strongly linked to the general ensemble characteristics of the particles, and might be more related to subpopulations or otherwise minor features of the sampled particles. Although it might be possible given large enough datasets to find more statistically relevant patterns from such methods, our results questions the overall feasibility of being able to capture the physicochemical properties governing immersion IN activity based on the on-line ensemble particle characterisation methods used by these studies.

Soot particles remain elusive with regard to their ability to act as INPs in the atmosphere, and further studies should focus on investigating IN activity more closely related to individual soot particle characteristics, such as by actually studying individual particles or by measuring more known homogeneous populations. Under many years, conflicting laboratory studies have reported soot to be anything from undetectable to efficient INPs. The challenges of comparing past soot particle IN studies lies in part in the lack of accompanying detailed physicochemical characterisation of the studied soot. It is otherwise very difficult to assess what type of particle is actually studied, as soot particle morphology and chemical composition can vary to a larger degree from smaller changes in combustion conditions. More recent studies seem to converge on the conclusion that soot is generally inefficient INPs (Vergara-Temprado et al., 2018; Kanji et al., 2020), questioning the relevance of including it in climate modelling studies. However, due to the very large quantities of different soot being released into the atmosphere, both naturally and anthropogenically, it is still of importance to fill the knowledge gap on the underlying mechanisms governing soot IN activity.

The combustion emissions from renewable diesel fuels HVO and RME using a modern heavy-duty diesel engine did not exhibit any increased immersion IN activity compared to a low-sulfur fossil fuel. A small increase in IN activity was observed from simulated atmospheric ageing of the low-sulfur fossil fuel emissions.

Measurements on modern heavy-duty diesel engine emissions are in agreement with the literature, identifying diesel combustion emissions as an inefficient source of INPs and not likely to be relevant for mixed-phase clouds (Chou et al., 2013; Schill et al., 2016). It is worth noting however, that diesel engines used in a laboratory setting represent only a subset of diesel engines and factors such as engine age, lubricants, maintenance and fuel quality may lead to different particle properties. To more conclusively assess the impact of diesel emissions it would be of value to also study diesel emissions for a range of such parameters related to real-life usage.

Combustion emissions from biomass-burning cook stoves were observed to have a moderate but discernible immersion IN activity under low-temperature MPC relevant conditions. Modifying combustion conditions towards less efficient combustion were in some cases observed to substantially increase the IN activity. While not explored in our work, previous research has linked inorganic elements to IN activity in biomass burning emissions (Petters et al., 2009). More recent studies have shown that mineralization of these compounds formed during combustion, and found on the soot particles is a reason for their immersion IN activity (Jahn et al., 2020), with atmospheric ageing potentially enhancing this effect (Jahl et al., 2021).

CCN properties of combustion emissions from biomass-burning cook stoves had a high variability, with a large dependence on stove design and type of fuel used. The CCN activity measured in κ decreased for increasing particle sizes in all experiments performed, and the κ for ultrafine mode particles increased with increasing combustion temperatures and was also observed to relate to the concentrations of potassium in the fuel. Large variations in primary CCN emission factors were mainly associated with fuel composition, and to a lesser extent the stove type. Simulated atmospheric ageing increased CCN emission factors for lower levels of supersaturation.

Biomass burning is likely to be of relevance for both CCN and INP concentrations in the atmosphere. Our findings coupled with the fact that emissions from residential biomass combustion constitutes a major part of global emissions, lead to a highly uncertain although likely significant regional and global source of CCN. A reduction in these emissions could, depending on factors such as importance relative to other CCN sources, lead to a climate-warming effect. However, biomass burning emissions already has a direct warming effect on the climate, and the current uncertainties regarding BrC in the atmosphere further complicates the question (Zeng et al., 2020). The observed dependence of CCN emissions on the fuel chemical composition found in the thesis work provides a promising pathway to estimate CCN emissions and should be developed further.

It is profoundly important to also consider the health aspects of biomass combustion emissions. Roughly half of the Earth's population, predominantly in developing regions, rely on traditional stoves and fuels for their everyday needs, which is linked to millions of premature deaths per year (HEI, 2020). The findings in this thesis show that it is possible to provide informed decisions on cook stove and fuel use from both a climate and health perspective, of potential aid to future policy measures. Although more research is needed in this regard, and additionally relies on many outstanding social, political and economic factors.

We are facing great and urgent challenges with regard to climate change, and while large uncertainties persist in our understanding of how combustion particles influence the climate we today know enough to reliably act on lowering our emissions of GHGs. Due to their prevalence in the atmosphere, however, our ability to establish efficient measures to mitigate climate change relies on understanding how combustion particles affect the climate both directly and indirectly through influencing cloud processes. This thesis work can be used to guide future work on understanding the fundamental mechanisms and larger scale implications of combustion particles on cloud processes.

7 Acknowledgements

I would like to start out by thanking Birgitta Svenningsson, my main supervisor, for always being supportive and understanding, and for all the interesting discussions and historical sidenotes through the years. Your knowledge and technical skill has always impressed.

Then i would like to thank my co-supervisor Thomas Kristensen. I could not thank you enough. You've been instrumental in me getting this far. I would also like to thank my co-supervisor Joakim Pagels. Your enthusiasm and knowledge on all-things-soot has been as enjoyable as it has been important. A huge thanks to all of you for your patience, and for helping me so much.

It's almost strange how many great people i've had the privilege of working alongside these years. Erik Ahlberg, thanks for letting a random master student mess around with your carefully planned experiment all those years ago, and for answering some thousand questions when i started. You too Cerina Wittbom, you guys were such a great help!

Stina Ausmeel, Karin Lovén, Malin Alsved, Jonas Jakobsson, Christina Andersen and Yuliya Omelekhina, thanks for all the great conference/courses/fika times we've had! Vilhelm Malmborg, thanks for all the above-and-beyond work you've contributed with, your knowledge has always impressed. And Louise Gren, you're such a great person and colleague, but foremost really, really good at your work and it's been such a great time sharing an office with you and Yuliya, thanks! And Lovisa Nilsson, thank you for all the excellent assistance during my measurements.

Thanks to all the other people over at division of Ergonomics and Aerosol Technology. Patrik Nilsson for putting so much good work in keeping the lab alive, and Axel Eriksson for trying to teach me about those mass spectrometry rodents.

Thanks to all the people over at the division of Nuclear Physics. Especially Charlotta Nilsson, Hanno Perrey and Göran Frank for doing so much to make teaching as easy as possible, and Yulia Lindholm and Jane Nilsson for being incredibly helpful on administrative matters. Pontus Roldin, Moa Sporre, Johan Friberg, thanks for all the interesting discussions! Adam Kristensson, you're a one of a kind selfless, caring person and it's been a pleasure working with you. Erik Swietlicki, thanks for introducing me to aerosol science!

Thanks to the people over as division of Combustion Physics. Per-Erik Bengtsson and Sandra Török, thanks for all the great help with creating soot!

Thanks to all the people at the Centre for Environment and Climate Science. Natascha Kljun, Ylva van Meeningen, Åsa-Katrin Erlandsson and Lina Nikoleris, for all your great work and the help you've given.

Thanks to Kimmo Korhonen at University of Eastern Finland for all the stimulating ice nucleating collaboration!

Thanks to the people over at Gothenburg University Department of Chemistry & Molecular Biology. Erik Thomson for all the interesting discussions, and casting a critical eye on my work. Nondas Tsiligiannis, Dimitri Castarede and Luis Filipe Escusa Dos Santos, always a pleasure hanging out with you guys!

Till sist, otroligt mycket tack till familj och vänner. Mormor Anna-Karin, du har alltid varit en så otroligt stark människa. Du har villkorslöst alltid varit där för mig, alltid trott på mig. Tack! Maria och Fredrik, och mina favoritkusiner Leonie och Anton, ni förtjänar också ett tack för allt! Anna, älskar dig! Tack för all skrivsupport Cecilia & Co! Joakim, Anna, Chibbe, Ditte, Jummy, Serena, CK, Robin, Rikard med flera; var skulle man vara utan er?

8 References

Abbatt, Jonathan P. D. (2003), 'Interactions of atmospheric trace gases with ice surfaces: adsorption and reaction', *Chemical Reviews* **103**(12), 4783–4800.
`https://doi.org/10.1021/cr0206418`

Andreae, M. O. and A. Gelencsér (2006), 'Black carbon or brown carbon? the nature of light-absorbing carbonaceous aerosols', *Atmospheric Chemistry and Physics* **6**(10), 3131–3148.
`https://doi.org/10.5194/acp-6-3131-2006`

Baldelli, Alberto, Una Trivanovic, Timothy A. Sipkens and Steven N. Rogak (2020), 'On determining soot maturity: A review of the role of microscopy- and spectroscopy-based techniques', *Chemosphere* **252**, 126532.
`https://doi.org/10.1016/j.chemosphere.2020.126532`

Bond, T. C., S. J. Doherty, D. W. Fahey, P. M. Forster, T. Berntsen, B. J. DeAngelo, M. G. Flanner, S. Ghan, B. Kärcher, D. Koch, S. Kinne, Y. Kondo, P. K. Quinn, M. C. Sarofim, M. G. Schultz, M. Schulz, C. Venkataraman, H. Zhang, S. Zhang, N. Bellouin, S. K. Guttikunda, P. K. Hopke, M. Z. Jacobson, J. W. Kaiser, Z. Klimont, U. Lohmann, J. P. Schwarz, D. Shindell, T. Storelvmo, S. G. Warren and C. S. Zender (2013), 'Bounding the role of black carbon in the climate system: A scientific assessment', *Journal of Geophysical Research: Atmospheres* **118**(11), 5380–5552.
`https://doi.org/10.1002/jgrd.50171`

Boucher, O., D. Randall, P. Artaxo, C. Bretherton, G. Feingold, P. Forster, V.-M. Kerminen, Y. Kondo, H. Liao, U. Lohmann, P. Rasch, S.K. Satheesh, S. Sherwood, B. Stevens and X.Y. Zhang (2013), *Clouds and Aerosols*, Cambridge University Press, Cambridge, United Kingdom and New York, NY, USA, book section 7, p. 571–658.
`www.climatechange2013.org`

Brooks, Sarah D., Katie Suter and Laura Olivarez (2014), 'Effects of chemical aging on the ice nucleation activity of soot and polycyclic aromatic hydrocarbon aerosols', *The Journal of Physical Chemistry A* **118**(43), 10036–10047.
`https://doi.org/10.1021/jp508809y`

Byčenkienė, Steigvilė, Vidmantas Ulevicius and Simonas Kecorius (2011), 'Characteristics of black carbon aerosol mass concentration over the east baltic region from two-year measurements', *Journal of Environmental Monitoring* **13**(4), 1027.
`https://doi.org/10.1039/c0em00480d`

Callendar, G. S. (1938), 'The artificial production of carbon dioxide and its influence on temperature', *Quarterly Journal of the Royal Meteorological Society* **64**(275), 223–240.
`https://doi.org/10.1002/qj.49706427503`

Campbell, James M. and Hugo K. Christenson (2018), 'Nucleation- and emergence-limited growth of ice from pores', *Physical Review Letters* **120**(16).
`https://doi.org/10.1103/physrevlett.120.165701`

Cantrell, Will and Andrew Heymsfield (2005), 'Production of ice in tropospheric clouds: A review', *Bulletin of the American Meteorological Society* **86**(6), 795–808.
`https://doi.org/10.1175/bams-86-6-795`

Cape, J.N., M. Coyle and P. Dumitrean (2012), 'The atmospheric lifetime of black carbon', *Atmospheric Environment* **59**, 256–263.
`https://doi.org/10.1016/j.atmosenv.2012.05.030`

Chou, C., Z. A. Kanji, O. Stetzer, T. Tritscher, R. Chirico, M. F. Heringa, E. Weingartner, A. S. H. Prévôt, U. Baltensperger and U. Lohmann (2013), 'Effect of photochemical ageing on the ice nucleation properties of diesel and wood burning particles', *Atmospheric Chemistry and Physics* **13**(2), 761–772.
`https://doi.org/10.5194/acp-13-761-2013`

Clougherty, Jane E. (2010), 'A growing role for gender analysis in air pollution epidemiology', *Environmental Health Perspectives* **118**(2), 167–176.
`https://doi.org/10.1289/ehp.0900994`

Corbin, J. C., U. Lohmann, B. Sierau, A. Keller, H. Burtscher and A. A. Mensah (2015), 'Black carbon surface oxidation and organic composition of beech-wood soot aerosols', *Atmospheric Chemistry and Physics* **15**(20), 11885–11907.
`https://doi.org/10.5194/acp-15-11885-2015`

Costa, Daniel L (2018), 'Historical highlights of air pollution toxicology', *Toxicological Sciences* **164**(1), 5–8.
`https://doi.org/10.1093/toxsci/kfy117`

Crutzen, Paul J. (2002), 'Geology of mankind', *Nature* **415**(6867), 23–23.
`https://doi.org/10.1038/415023a`

David, Robert O., Claudia Marcolli, Jonas Fahrni, Yuqing Qiu, Yamila A. Perez Sirkin, Valeria Molinero, Fabian Mahrt, Dominik Brühwiler, Ulrike Lohmann and Zamin A. Kanji (2019), 'Pore condensation and freezing is responsible for ice formation below water saturation for porous particles', *Proceedings of the National Academy of Sciences* **116**(17), 8184–8189.
`https://doi.org/10.1073/pnas.1813647116`

David, Robert O., Jonas Fahrni, Claudia Marcolli, Fabian Mahrt, Dominik Brühwiler and Zamin A. Kanji (2020), 'The role of contact angle and pore width on pore condensation and freezing', *Atmospheric Chemistry and Physics* **20**(15), 9419–9440.
`https://doi.org/10.5194/acp-20-9419-2020`

Davies, James F., Andreas Zuend and Kevin R. Wilson (2019), 'Technical note: The role of evolving surface tension in the formation of cloud droplets', *Atmospheric Chemistry and Physics* **19**(5), 2933–2946.
`https://doi.org/10.5194/acp-19-2933-2019`

de Boer, G., H. Morrison, M. D. Shupe and R. Hildner (2011), 'Evidence of liquid dependent ice nucleation in high-latitude stratiform clouds from surface remote sensors', *Geophysical Research Letters* **38**(1), n/a–n/a.
`https://doi.org/10.1029/2010gl046016`

DeMott, P. J., A. J. Prenni, X. Liu, S. M. Kreidenweis, M. D. Petters, C. H. Twohy, M. S. Richardson, T. Eidhammer and D. C. Rogers (2010), 'Predicting global atmospheric ice nuclei distributions and their impacts on climate', *Proceedings of the National Academy of Sciences* **107**(25), 11217–11222.
`https://doi.org/10.1073/pnas.0910818107`

DeMott, P. J., Y. Chen, S. M. Kreidenweis, D. C. Rogers and D. E. Sherman (1999), 'Ice formation by black carbon particles', *Geophysical Research Letters* **26**(16), 2429–2432.
`https://doi.org/10.1029/1999gl900580`

DeMott, Paul J. (1990), 'An exploratory study of ice nucleation by soot aerosols', *Journal of Applied Meteorology* **29**(10), 1072–1079.
`https://doi.org/10.1175/1520-0450(1990)029<1072:aesoin>2.0.co;2`

Diehl, K. and S.K. Mitra (1998), 'A laboratory study of the effects of a kerosene-burner exhaust on ice nucleation and the evaporation rate of ice crystals', *Atmospheric Environment* **32**(18), 3145–3151.
`https://doi.org/10.1016/s1352-2310(97)00467-6`

Dockery, Douglas W., C. Arden Pope, Xiping Xu, John D. Spengler, James H. Ware, Martha E. Fay, Benjamin G. Ferris and Frank E. Speizer (1993), 'An association between air pollution and mortality in six u.s. cities', *New England Journal of Medicine* **329**(24), 1753–1759.
`https://doi.org/10.1056/nejm199312093292401`

Durant, Adam J. (2005), 'Evaporation freezing by contact nucleation inside-out', *Geophysical Research Letters* **32**(20).
`https://doi.org/10.1029/2005gl024175`

Dymarska, Magdalena, Benjamin J. Murray, Limin Sun, Michael L. Eastwood, Daniel A. Knopf and Allan K. Bertram (2006), 'Deposition ice nucleation on soot at temperatures relevant for the lower troposphere', *Journal of Geophysical Research* **111**(D4).
`https://doi.org/10.1029/2005jd006627`

ESMAP (2020), *The State of Access to Modern Energy Cooking Services (English)*, World Bank, World Bank, Washington, D.C.
`http://hdl.handle.net/10986/34565`

Figueiredo, J.L, M.F.R Pereira, M.M.A Freitas and J.J.M Órfão (1999), 'Modification of the surface chemistry of activated carbons', *Carbon* **37**(9), 1379–1389.
`https://doi.org/10.1016/s0008-6223(98)00333-9`

Forouzanfar, Mohammad H, Ashkan Afshin, Lily T Alexander, H Ross Anderson, Zulfiqar A Bhutta, Stan Biryukov, ... and Christopher J L Murray (2016), 'Global, regional, and national comparative risk assessment of 79 behavioural, environmental and occupational, and metabolic risks or clusters of risks, 1990–2015: a systematic analysis for the global burden of disease study 2015', *The Lancet* **388**(10053), 1659–1724.
`https://doi.org/10.1016/s0140-6736(16)31679-8`

Fowler, Kathryn, Paul Connolly and David Topping (2020), 'Modelling the effect of condensed-phase diffusion on the homogeneous nucleation of ice in ultra-viscous particles', *Atmospheric Chemistry and Physics* **20**(2), 683–698.
`https://doi.org/10.5194/acp-20-683-2020`

Frenklach, Michael (2002), 'Reaction mechanism of soot formation in flames', *Physical Chemistry Chemical Physics* **4**(11), 2028–2037.
`https://doi.org/10.1039/b110045a`

Frenklach, Michael and Alexander M. Mebel (2020), 'On the mechanism of soot nucleation', *Physical Chemistry Chemical Physics* **22**(9), 5314–5331.
`https://doi.org/10.1039/d0cp00116c`

Friedman, Beth, Gourihar Kulkarni, Josef Beránek, Alla Zelenyuk, Joel A. Thornton and Daniel J. Cziczo (2011), 'Ice nucleation and droplet formation by bare and coated soot particles', *Journal of Geophysical Research* **116**(D17).
`https://doi.org/10.1029/2011jd015999`

Gallo, Yann, Vilhelm B. Malmborg, Johan Simonsson, Erik Svensson, MengQin Shen, Per-Erik Bengtsson, Joakim Pagels, Martin Tunér, Antonio Garcia and Öivind Andersson (2017), 'Investigation of late-cycle soot oxidation using laser extinction and in-cylinder gas sampling at varying inlet oxygen concentrations in

diesel engines', *Fuel* **193**, 308–314.
`https://doi.org/10.1016/j.fuel.2016.12.013`

Garimella, Sarvesh, Thomas Bjerring Kristensen, Karolina Ignatius, Andre Welti, Jens Voigtländer, Gourihar R. Kulkarni, Frank Sagan, Gregory Lee Kok, James Dorsey, Leonid Nichman, Daniel Alexander Rothenberg, Michael Rösch, Amélie Catharina Ruth Kirchgäßner, Russell Ladkin, Heike Wex, Theodore W. Wilson, Luis Antonio Ladino, Jon P. D. Abbatt, Olaf Stetzer, Ulrike Lohmann, Frank Stratmann and Daniel James Cziczo (2016), 'The SPectrometer for ice nuclei (SPIN): an instrument to investigate ice nucleation', *Atmospheric Measurement Techniques* **9**(7), 2781–2795.
`https://doi.org/10.5194/amt-9-2781-2016`

Glassman, Irvin (1989), 'Soot formation in combustion processes', *Symposium (International) on Combustion* **22**(1), 295–311.
`https://doi.org/10.1016/s0082-0784(89)80036-0`

Goto-Azuma, K., M. Hirabayashi, H. Motoyama, T. Miyake, T. Kuramoto, R. Uemura, M. Igarashi, Y. Iizuka, T. Sakurai, S. Horikawa, K. Suzuki, T. Suzuki, K. Fujita, Y. Kondo, S. Hattori and Y. Fujii (2019), 'Reduced marine phytoplankton sulphur emissions in the southern ocean during the past seven glacials', *Nature Communications* **10**(1).
`https://doi.org/10.1038/s41467-019-11128-6`

Gysel, M., E. Weingartner and U. Baltensperger (2002), 'Hygroscopicity of aerosol particles at low temperatures. 2. theoretical and experimental hygroscopic properties of laboratory generated aerosols', *Environmental Science & Technology* **36**(1), 63–68.
`https://doi.org/10.1021/es010055g`

Halpern, Benjamin S., Shaun Walbridge, Kimberly A. Selkoe, Carrie V. Kappel, Fiorenza Micheli, Caterina D'Agrosa, John F. Bruno, Kenneth S. Casey, Colin Ebert, Helen E. Fox, Rod Fujita, Dennis Heinemann, Hunter S. Lenihan, Elizabeth M. P. Madin, Matthew T. Perry, Elizabeth R. Selig, Mark Spalding, Robert Steneck and Reg Watson (2008), 'A global map of human impact on marine ecosystems', *Science* **319**(5865), 948–952.
`https://doi.org/10.1126/science.1149345`

Hande, Luke B. and Corinna Hoose (2017), 'Partitioning the primary ice formation modes in large eddy simulations of mixed-phase clouds', *Atmospheric Chemistry and Physics* **17**(22), 14105–14118.
`https://doi.org/10.5194/acp-17-14105-2017`

Harris, Stephen J. and Anita M. Weiner (1983), 'Surface growth of soot particles in premixed ethylene/air flames', *Combustion Science and Technology* **31**(3-4), 155–167.
`https://doi.org/10.1080/00102208308923637`

HEI (2020), *State of Global Air 2020. Special Report*, Health Effects Institute, Health Effects Institute, Boston, MA.
`https://www.stateofglobalair.org/resources`

Heymsfield, Andrew J., Martina Krämer, Anna Luebke, Phil Brown, Daniel J. Cziczo, Charmaine Franklin, Paul Lawson, Ulrike Lohmann, Greg McFarquhar, Zbigniew Ulanowski and Kristof Van Tricht (2017), 'Cirrus clouds', *Meteorological Monographs* **58**, 2.1–2.26.
`https://doi.org/10.1175/amsmonographs-d-16-0010.1`

Hodzic, Alma, Pedro Campuzano-Jost, Huisheng Bian, Mian Chin, Peter R. Colarco, Douglas A. Day, Karl D. Froyd, Bernd Heinold, Duseong S. Jo, Joseph M. Katich, John K. Kodros, Benjamin A. Nault, Jeffrey R.

Pierce, Eric Ray, Jacob Schacht, Gregory P. Schill, Jason C. Schroder, Joshua P. Schwarz, Donna T. Sueper, Ina Tegen, Simone Tilmes, Kostas Tsigaridis, Pengfei Yu and Jose L. Jimenez (2020), 'Characterization of organic aerosol across the global remote troposphere: a comparison of ATom measurements and global chemistry models', *Atmospheric Chemistry and Physics* **20**(8), 4607–4635.
`https://doi.org/10.5194/acp-20-4607-2020`

Homann, Klaus-Heinrich (1998), 'Fullerenes and soot formation— new pathways to large particles in flames', *Angewandte Chemie International Edition* **37**(18), 2434–2451.
`https://doi.org/10.1002/(sici)1521-3773(19981002)37:18<2434::aid-anie2434>3.0.co;2-l`

Hoose, C. and O. Möhler (2012), 'Heterogeneous ice nucleation on atmospheric aerosols: a review of results from laboratory experiments', *Atmospheric Chemistry and Physics* **12**(20), 9817–9854.
`https://doi.org/10.5194/acp-12-9817-2012`

IEA (2014), *World Energy Outlook 2014*, IEA, Paris.
`https://www.oecd-ilibrary.org/content/publication/weo-2014-en`

IEA, IRENA, UNSD, World Bank and WHO (2020), *Tracking SDG 7: The Energy Progress Report*, World Bank, World Bank, Washington, D.C.
`https://www.iea.org/reports/tracking-sdg7-the-energy-progress-report-2020`

IPCC (2013), *Summary for Policymakers*, Cambridge University Press, Cambridge, United Kingdom and New York, NY, USA, book section SPM, p. 1–30.
`www.climatechange2013.org`

Jahl, Lydia G., Thomas A. Brubaker, Michael J. Polen, Leif G. Jahn, Kerrigan P. Cain, Bailey B. Bowers, William D. Fahy, Sara Graves and Ryan C. Sullivan (2021), 'Atmospheric aging enhances the ice nucleation ability of biomass-burning aerosol', *Science Advances* 7(9), eabd3440.
`https://doi.org/10.1126/sciadv.abd3440`

Jahn, Leif G., Michael J. Polen, Lydia G. Jahl, Thomas A. Brubaker, Joshua Somers and Ryan C. Sullivan (2020), 'Biomass combustion produces ice-active minerals in biomass-burning aerosol and bottom ash', *Proceedings of the National Academy of Sciences* **117**(36), 21928–21937.
`https://doi.org/10.1073/pnas.1922128117`

Johansson, K. O., M. P. Head-Gordon, P. E. Schrader, K. R. Wilson and H. A. Michelsen (2018), 'Resonance-stabilized hydrocarbon-radical chain reactions may explain soot inception and growth', *Science* **361**(6406), 997–1000.
`https://doi.org/10.1126/science.aat3417`

Kanakidou, M., J. H. Seinfeld, S. N. Pandis, I. Barnes, F. J. Dentener, M. C. Facchini, R. Van Dingenen, B. Ervens, A. Nenes, C. J. Nielsen, E. Swietlicki, J. P. Putaud, Y. Balkanski, S. Fuzzi, J. Horth, G. K. Moortgat, R. Winterhalter, C. E. L. Myhre, K. Tsigaridis, E. Vignati, E. G. Stephanou and J. Wilson (2005), 'Organic aerosol and global climate modelling: a review', *Atmospheric Chemistry and Physics* **5**(4), 1053–1123.
`https://doi.org/10.5194/acp-5-1053-2005`

Kanji, Z. A., P. J. DeMott, O. Möhler and J. P. D. Abbatt (2011), 'Results from the university of toronto continuous flow diffusion chamber at ICIS 2007: instrument intercomparison and ice onsets for different aerosol types', *Atmospheric Chemistry and Physics* **11**(1), 31–41.
`https://doi.org/10.5194/acp-11-31-2011`

Kanji, Zamin A., André Welti, Joel C. Corbin and Amewu A. Mensah (2020), ‘Black carbon particles do not matter for immersion mode ice nucleation’, *Geophysical Research Letters* **47**(11).
`https://doi.org/10.1029/2019gl086764`

Kanji, Zamin A., Luis A. Ladino, Heike Wex, Yvonne Boose, Monika Burkert-Kohn, Daniel J. Cziczo and Martina Krämer (2017), ‘Overview of ice nucleating particles’, *Meteorological Monographs* **58**, 1.1–1.33.
`https://doi.org/10.1175/amsmonographs-d-16-0006.1`

Kärcher, Bernd (2018), ‘Formation and radiative forcing of contrail cirrus’, *Nature Communications* **9**(1).
`https://doi.org/10.1038/s41467-018-04068-0`

Keeling, Charles D. (1973), ‘Industrial production of carbon dioxide from fossil fuels and limestone’, *Tellus* **25**(2), 174–198.
`https://doi.org/10.1111/j.2153-3490.1973.tb01604.x`

Keeling, Charles D., Robert B. Bacastow, Arnold E. Bainbridge, Carl A. Ekdahl Jr., Peter R. Guenther, Lee S. Waterman and John F. S. Chin (1976), ‘Atmospheric carbon dioxide variations at mauna loa observatory, hawaii’, *Tellus* **28**(6), 538–551.
`https://doi.org/10.3402/tellusa.v28i6.11322`

Kholghy, Mohammad Reza, Armin Veshkini and Murray John Thomson (2016), ‘The core–shell internal nanostructure of soot – a criterion to model soot maturity’, *Carbon* **100**, 508–536.
`https://doi.org/10.1016/j.carbon.2016.01.022`

Klimont, Zbigniew, Kaarle Kupiainen, Chris Heyes, Pallav Purohit, Janusz Cofala, Peter Rafaj, Jens Borken-Kleefeld and Wolfgang Schöpp (2017), ‘Global anthropogenic emissions of particulate matter including black carbon’, *Atmospheric Chemistry and Physics* **17**(14), 8681–8723.
`https://doi.org/10.5194/acp-17-8681-2017`

Knopf, Daniel A., Peter A. Alpert and Bingbing Wang (2018), ‘The role of organic aerosol in atmospheric ice nucleation: A review’, *ACS Earth and Space Chemistry* **2**(3), 168–202.
`https://doi.org/10.1021/acsearthspacechem.7b00120`

Koehler, Kirsten A., Paul J. DeMott, Sonia M. Kreidenweis, Olga B. Popovicheva, Markus D. Petters, Christian M. Carrico, Elena D. Kireeva, Tatiana D. Khokhlova and Natalia K. Shonija (2009), ‘Cloud condensation nuclei and ice nucleation activity of hydrophobic and hydrophilic soot particles’, *Physical Chemistry Chemical Physics* **11**(36), 7906.
`https://doi.org/10.1039/b905334b`

Köhler, Hilding (1936), ‘The nucleus in and the growth of hygroscopic droplets’, *Trans. Faraday Soc.* **32**(0), 1152–1161.
`https://doi.org/10.1039/tf9363201152`

Korolev, A., G. McFarquhar, P. R. Field, C. Franklin, P. Lawson, Z. Wang, E. Williams, S. J. Abel, D. Axisa, S. Borrmann, J. Crosier, J. Fugal, M. Krämer, U. Lohmann, O. Schlenczek, M. Schnaiter and M. Wendisch (2017), ‘Mixed-phase clouds: Progress and challenges’, *Meteorological Monographs* **58**, 5.1–5.50.
`https://doi.org/10.1175/amsmonographs-d-17-0001.1`

Korolev, Alexei and Thomas Leisner (2020), ‘Review of experimental studies of secondary ice production’, *Atmospheric Chemistry and Physics* **20**(20), 11767–11797.
`https://doi.org/10.5194/acp-20-11767-2020`

Kulkarni, Gourihar, Swarup China, Shang Liu, Manjula Nandasiri, Noopur Sharma, Jacqueline Wilson, Allison C. Aiken, Duli Chand, Alexander Laskin, Claudio Mazzoleni, Mikhail Pekour, John Shilling, Vaithiyalingam Shutthanandan, Alla Zelenyuk and Rahul A. Zaveri (2016), 'Ice nucleation activity of diesel soot particles at cirrus relevant temperature conditions: Effects of hydration, secondary organics coating, soot morphology, and coagulation', *Geophysical Research Letters* **43**(7), 3580–3588.
`https://doi.org/10.1002/2016gl068707`

Kulmala, Markku, Ari Laaksonen, Robert J.Charlson and Pekka Korhonen (1997), 'Clouds without supersaturation', *Nature* **388**(6640), 336–337.
`https://doi.org/10.1038/41000`

Laaksonen, Ari, Pekka Korhonen, Markku Kulmala and Robert J. Charlson (1998), 'Modification of the köhler equation to include soluble trace gases and slightly soluble substances', *Journal of the Atmospheric Sciences* **55**(5), 853–862.
`https://doi.org/10.1175/1520-0469(1998)055<0853:motkhe>2.0.co;2`

Lacey, Forrest G., Daven K. Henze, Colin J. Lee, Aaron van Donkelaar and Randall V. Martin (2017), 'Transient climate and ambient health impacts due to national solid fuel cookstove emissions', *Proceedings of the National Academy of Sciences* **114**(6), 1269–1274.
`https://doi.org/10.1073/pnas.1612430114`

Lack, D. A., R. Bahreini, J. M. Langridge, J. B. Gilman and A. M. Middlebrook (2013), 'Brown carbon absorption linked to organic mass tracers in biomass burning particles', *Atmospheric Chemistry and Physics* **13**(5), 2415–2422.
`https://doi.org/10.5194/acp-13-2415-2013`

Lahaye, J. and G. Prado (1981), Morphology and internal structure of soot and carbon blacks, *in* 'Particulate Carbon', Springer US, pp. 33–55.
`https://doi.org/10.1007/978-1-4757-6137-5_2`

Landrigan, Philip J, Richard Fuller, Nereus J R Acosta, Olusoji Adeyi, Robert Arnold, Niladri (Nil) Basu, ... and Ma Zhong (2018), 'The lancet commission on pollution and health', *The Lancet* **391**(10119), 462–512.
`https://doi.org/10.1016/s0140-6736(17)32345-0`

Laskin, Alexander, Julia Laskin and Sergey A. Nizkorodov (2015), 'Chemistry of atmospheric brown carbon', *Chemical Reviews* **115**(10), 4335–4382.
`https://doi.org/10.1021/cr5006167`

Liu, Yongchun, Chang Liu, Jinzhu Ma, Qingxin Ma and Hong He (2010), 'Structural and hygroscopic changes of soot during heterogeneous reaction with o3', *Physical Chemistry Chemical Physics* **12**(36), 10896.
`https://doi.org/10.1039/c0cp00402b`

Lübken, Franz-Josef, Uwe Berger and Gerd Baumgarten (2018), 'On the anthropogenic impact on long-term evolution of noctilucent clouds', *Geophysical Research Letters* **45**(13), 6681–6689.
`https://doi.org/10.1029/2018gl077719`

Lund, Marianne T., Bjørn H. Samset, Ragnhild B. Skeie, Duncan Watson-Parris, Joseph M. Katich, Joshua P. Schwarz and Bernadett Weinzierl (2018), 'Short black carbon lifetime inferred from a global set of aircraft observations', *npj Climate and Atmospheric Science* **1**(1).
`https://doi.org/10.1038/s41612-018-0040-x`

Mahrt, Fabian, Claudia Marcolli, Robert O. David, Philippe Grönquist, Eszter J. Barthazy Meier, Ulrike Lohmann and Zamin A. Kanji (2018), 'Ice nucleation abilities of soot particles determined with the horizontal ice nucleation chamber', *Atmospheric Chemistry and Physics* **18**(18), 13363–13392.
`https://doi.org/10.5194/acp-18-13363-2018`

Malmborg, Vilhelm B., Axel C. Eriksson, Sandra Török, Yilong Zhang, Kirsten Kling, Johan Martinsson, Edward C. Fortner, Louise Gren, Sanghoon Kook, Timothy B. Onasch, Per-Erik Bengtsson and Joakim Pagels (2019), 'Relating aerosol mass spectra to composition and nanostructure of soot particles', *Carbon* **142**, 535–546.
`https://doi.org/10.1016/j.carbon.2018.10.072`

Marcolli, C. (2014), 'Deposition nucleation viewed as homogeneous or immersion freezing in pores and cavities', *Atmospheric Chemistry and Physics* **14**(4), 2071–2104.
`https://doi.org/10.5194/acp-14-2071-2014`

Moffet, R. C. and K. A. Prather (2009), 'In-situ measurements of the mixing state and optical properties of soot with implications for radiative forcing estimates', *Proceedings of the National Academy of Sciences* **106**(29), 11872–11877.
`https://doi.org/10.1073/pnas.0900040106`

Möhler, O. (2005), 'Effect of sulfuric acid coating on heterogeneous ice nucleation by soot aerosol particles', *Journal of Geophysical Research* **110**(D11).
`https://doi.org/10.1029/2004jd005169`

Moore, Richard H. and Athanasios Nenes (2009), 'Scanning flow CCN analysis—a method for fast measurements of CCN spectra', *Aerosol Science and Technology* **43**(12), 1192–1207.
`https://doi.org/10.1080/02786820903289780`

Mülmenstädt, Johannes, O. Sourdeval, J. Delanoë and J. Quaas (2015), 'Frequency of occurrence of rain from liquid-, mixed-, and ice-phase clouds derived from a-train satellite retrievals', *Geophysical Research Letters* **42**(15), 6502–6509.
`https://doi.org/10.1002/2015gl064604`

Murray, B. J., D. O'Sullivan, J. D. Atkinson and M. E. Webb (2012), 'Ice nucleation by particles immersed in supercooled cloud droplets', *Chemical Society Reviews* **41**(19), 6519.
`https://doi.org/10.1039/c2cs35200a`

Myhre, G., D. Shindell, F.-M. Bréon, W. Collins, J. Fuglestvedt, J. Huang, D. Koch, J.-F. Lamarque, D. Lee, B. Mendoza, T. Nakajima, A. Robock, G. Stephens, T. Takemura and H. Zhang (2013), *Anthropogenic and Natural Radiative Forcing*, Cambridge University Press, Cambridge, United Kingdom and New York, NY, USA, book section 8, p. 659–740.
`www.climatechange2013.org`

Nagare, Baban, Claudia Marcolli, André Welti, Olaf Stetzer and Ulrike Lohmann (2016), 'Comparing contact and immersion freezing from continuous flow diffusion chambers', *Atmospheric Chemistry and Physics* **16**(14), 8899–8914.
`https://doi.org/10.5194/acp-16-8899-2016`

Niehaus, Joseph and Will Cantrell (2015), 'Contact freezing of water by salts', *The Journal of Physical Chemistry Letters* **6**(17), 3490–3495.
`https://doi.org/10.1021/acs.jpclett.5b01531`

Pales, Jack C. and Charles D. Keeling (1965), 'The concentration of atmospheric carbon dioxide in hawaii', *Journal of Geophysical Research* **70**(24), 6053–6076.
`https://doi.org/10.1029/jz070i024p06053`

Petters, M. D. and S. M. Kreidenweis (2007), 'A single parameter representation of hygroscopic growth and cloud condensation nucleus activity', *Atmospheric Chemistry and Physics* **7**(8), 1961–1971.
`https://doi.org/10.5194/acp-7-1961-2007`

Petters, M. D. and S. M. Kreidenweis (2013), 'A single parameter representation of hygroscopic growth and cloud condensation nucleus activity – part 3: Including surfactant partitioning', *Atmospheric Chemistry and Physics* **13**(2), 1081–1091.
`https://doi.org/10.5194/acp-13-1081-2013`

Petters, Markus D., Matthew T. Parsons, Anthony J. Prenni, Paul J. DeMott, Sonia M. Kreidenweis, Christian M. Carrico, Amy P. Sullivan, Gavin R. McMeeking, Ezra Levin, Cyle E. Wold, Jeffrey L. Collett and Hans Moosmüller (2009), 'Ice nuclei emissions from biomass burning', *Journal of Geophysical Research* **114**(D7).
`https://doi.org/10.1029/2008jd011532`

Popovicheva, O. B., N. M. Persiantseva, E. E. Lukhovitskaya, N. K. Shonija, N. A. Zubareva, B. Demirdjian, D. Ferry and J. Suzanne (2004), 'Aircraft engine soot as contrail nuclei', *Geophysical Research Letters* **31**(11), n/a–n/a.
`https://doi.org/10.1029/2003gl018888`

Prisle, N. L., T. Raatikainen, A. Laaksonen and M. Bilde (2010), 'Surfactants in cloud droplet activation: mixed organic-inorganic particles', *Atmospheric Chemistry and Physics* **10**(12), 5663–5683.
`https://doi.org/10.5194/acp-10-5663-2010`

Ramanathan, V. and G. Carmichael (2008), 'Global and regional climate changes due to black carbon', *Nature Geoscience* **1**(4), 221–227.
`https://doi.org/10.1038/ngeo156`

Rhein, M., S.R. Rintoul, S. Aoki, E. Campos, D. Chambers, R.A. Feely, S. Gulev, G.C. Johnson, S.A. Josey, A. Kostianoy, C. Mauritzen, D. Roemmich, L.D. Talley and F. Wang (2013), *Observations: Ocean*, Cambridge University Press, Cambridge, United Kingdom and New York, NY, USA, book section 3, p. 255–316.
`www.climatechange2013.org`

Richter, H and J.B Howard (2000), 'Formation of polycyclic aromatic hydrocarbons and their growth to soot—a review of chemical reaction pathways', *Progress in Energy and Combustion Science* **26**(4-6), 565–608.
`https://doi.org/10.1016/s0360-1285(00)00009-5`

Rissler, J., A. Vestin, E. Swietlicki, G. Fisch, J. Zhou, P. Artaxo and M. O. Andreae (2006), 'Size distribution and hygroscopic properties of aerosol particles from dry-season biomass burning in amazonia', *Atmospheric Chemistry and Physics* **6**(2), 471–491.
`https://doi.org/10.5194/acp-6-471-2006`

Rissler, Jenny (2005), Hygroscopic Properties of Aerosols from Open-Air Burning and Controlled Combustion of Biomass, PhD thesis, Lund University.

Rodhe, Henning, Christer Persson and Ove Åkesson (1972), 'An investigation into regional transport of soot and sulfate aerosols', *Atmospheric Environment (1967)* **6**(9), 675–693.
`https://doi.org/10.1016/0004-6981(72)90025-x`

Saathoff, H., K.-H. Naumann, M. Schnaiter, W. Schöck, O. Möhler, U. Schurath, E. Weingartner, M. Gysel and U. Baltensperger (2003), 'Coating of soot and (NH4)2so4 particles by ozonolysis products of α-pinene', *Journal of Aerosol Science* **34**(10), 1297–1321.
`https://doi.org/10.1016/s0021-8502(03)00364-1`

Schill, G. P., S. H. Jathar, J. K. Kodros, E. J. T. Levin, A. M. Galang, B. Friedman, M. F. Link, D. K. Farmer, J. R. Pierce, S. M. Kreidenweis and P. J. DeMott (2016), 'Ice-nucleating particle emissions from photochemically aged diesel and biodiesel exhaust', *Geophysical Research Letters* **43**(10), 5524–5531.
`https://doi.org/10.1002/2016gl069529`

Smith, Kirk R., Nigel Bruce, Kalpana Balakrishnan, Heather Adair-Rohani, John Balmes, Zoë Chafe, Mukesh Dherani, H. Dean Hosgood, Sumi Mehta, Daniel Pope and Eva Rehfuess (2014), 'Millions dead: How do we know and what does it mean? methods used in the comparative risk assessment of household air pollution', *Annual Review of Public Health* **35**(1), 185–206.
`https://doi.org/10.1146/annurev-publhealth-032013-182356`

Smith, Owen I. (1981), 'Fundamentals of soot formation in flames with application to diesel engine particulate emissions', *Progress in Energy and Combustion Science* 7(4), 275–291.
`https://doi.org/10.1016/0360-1285(81)90002-2`

Topping, D. O., G. B. McFiggans and H. Coe (2005), 'A curved multi-component aerosol hygroscopicity model framework: Part 2 – including organic compounds', *Atmospheric Chemistry and Physics* **5**(5), 1223–1242.
`https://doi.org/10.5194/acp-5-1223-2005`

Tree, Dale R. and Kenth I. Svensson (2007), 'Soot processes in compression ignition engines', *Progress in Energy and Combustion Science* **33**(3), 272–309.
`https://doi.org/10.1016/j.pecs.2006.03.002`

Tritscher, Ines, Michael C. Pitts, Lamont R. Poole, Simon P. Alexander, Francesco Cairo, Martyn P. Chipperfield, Jens-Uwe Grooß, Michael Höpfner, Alyn Lambert, Beiping Luo, Sergey Molleker, Andrew Orr, Ross Salawitch, Marcel Snels, Reinhold Spang, Wolfgang Woiwode and Thomas Peter (2021), 'Polar stratospheric clouds: Satellite observations, processes, and role in ozone depletion', *Reviews of Geophysics* **59**(2).
`https://doi.org/10.1029/2020rg000702`

Ullrich, Romy, Corinna Hoose, Ottmar Möhler, Monika Niemand, Robert Wagner, Kristina Höhler, Naruki Hiranuma, Harald Saathoff and Thomas Leisner (2017), 'A new ice nucleation active site parameterization for desert dust and soot', *Journal of the Atmospheric Sciences* **74**(3), 699–717.
`https://doi.org/10.1175/jas-d-16-0074.1`

UN. Secretary-General (2020), *Progress towards the Sustainable Development Goals : report of the Secretary-General (Report No. E/2020/57)*, United Nations, New York.
`https://digitallibrary.un.org/record/3865828?ln=en`

Vali, G., P. J. DeMott, O. Möhler and T. F. Whale (2015), 'Technical note: A proposal for ice nucleation terminology', *Atmospheric Chemistry and Physics* **15**(18), 10263–10270.
`https://doi.org/10.5194/acp-15-10263-2015`

Vergara-Temprado, Jesús, Mark A. Holden, Thomas R. Orton, Daniel O'Sullivan, Nsikanabasi S. Umo, Jo Browse, Carly Reddington, María Teresa Baeza-Romero, Jenny M. Jones, Amanda Lea-Langton, Alan Williams, Ken S. Carslaw and Benjamin J. Murray (2018), 'Is black carbon an unimportant ice-nucleating particle in mixed-phase clouds?', *Journal of Geophysical Research: Atmospheres* **123**(8), 4273–4283.
`https://doi.org/10.1002/2017jd027831`

Wang, Hai (2011), ‘Formation of nascent soot and other condensed-phase materials in flames’, *Proceedings of the Combustion Institute* **33**(1), 41–67.
`https://doi.org/10.1016/j.proci.2010.09.009`

WHO (2016), *Ambient air pollution: a global assessment of exposure and burden of disease*, World Health Organization.
`https://apps.who.int/iris/handle/10665/250141`

World Bank (2014), *The World Bank Annual Report 2014*, The World Bank.
`https://doi.org/10.1596/978-1-4648-0245-4`

Xue, Huaxin, Alexei F. Khalizov, Lin Wang, Jun Zheng and Renyi Zhang (2009), ‘Effects of dicarboxylic acid coating on the optical properties of soot’, *Physical Chemistry Chemical Physics* **11**(36), 7869.
`https://doi.org/10.1039/b904129j`

Zeng, Linghan, Aoxing Zhang, Yuhang Wang, Nicholas L. Wagner, Joseph M. Katich, Joshua P. Schwarz, Gregory P. Schill, Charles Brock, Karl D. Froyd, Daniel M. Murphy, Christina J. Williamson, Agnieszka Kupc, Eric Scheuer, Jack Dibb and Rodney J. Weber (2020), ‘Global measurements of brown carbon and estimated direct radiative effects’, *Geophysical Research Letters* **47**(13).
`https://doi.org/10.1029/2020gl088747`

Zhang, R., A. F. Khalizov, J. Pagels, D. Zhang, H. Xue and P. H. McMurry (2008), ‘Variability in morphology, hygroscopicity, and optical properties of soot aerosols during atmospheric processing’, *Proceedings of the National Academy of Sciences* **105**(30), 10291–10296.
`https://doi.org/10.1073/pnas.0804860105`

Zhang, Yuzhong, Haviland Forrister, Jiumeng Liu, Jack Dibb, Bruce Anderson, Joshua P. Schwarz, Anne E. Perring, Jose L. Jimenez, Pedro Campuzano-Jost, Yuhang Wang, Athanasios Nenes and Rodney J. Weber (2017), ‘Top-of-atmosphere radiative forcing affected by brown carbon in the upper troposphere’, *Nature Geoscience* **10**(7), 486–489.
`https://doi.org/10.1038/ngeo2960`